# Dynamic Analysis of Beam Structures under Moving Loads: A Review of the Modal Expansion Method

**Z. Dimitrovová**
**UNIC, Department of Civil Engineering**
**Universidade Nova de Lisboa, Portugal**

in B.H.V. Topping and Y. Tsompanakis, (Editor), "Civil and Structural Engineering Computational Technology", Saxe-Coburg Publications, Stirlingshire, UK, Chapter 4, pp 99-130, 2011. doi:10.4203/csets.28.4

## Abstract

In this chapter, the dynamic analysis of beam structures under moving loads is presented. Hamilton's principle is implemented as an efficient tool for obtaining the governing equations for transversal vibrations in beam structures induced by moving loads. The determination of elastic constants representing the effect of an elastic half space is included. The influence of the axial force is also considered. The concept of the dynamic stiffness matrix is posted as a general principle for finite, semi-infinite and infinite beams. Its implementation in beam structures composed of several sub-domains is developed. Advantages and disadvantages of modal expansion in series governed by damped and undamped modes are stated.

**Keywords:** dynamic stiffness matrix, state-space formulation, moving load, moving mass, modal expansion, localized disturbances.

## 1 Introduction

Dynamic analyses of beam structures under moving loads have attracted the engineering and scientific community from the middle of the 19th century, when railway construction began. Several concerns related to railway lines can be quickly solved on simple models concerning just a beam on a viscoelastic foundation traversed by uniformly moving loads. Since a considerable amount of studies have been published on this subject, only a few pioneering works are mentioned. Dynamic stresses in the beam structure were firstly solved by Krylov [1] and later by Timoshenko [2]. Transversal vibrations in a simply supported beam traversed by a constant force moving at a constant velocity were presented by Inglis [3], Lowan [4] and later on, other solutions have been given by Koloušek [5] and Frýba [6]. These works employ mainly modal expansion methods. The first solutions for infinite beams were presented by Timoshenko [7]. In [8] the effect of viscous damping in the foundation is discussed. The case of a load variable in time is presented in [9].

The first high speed line, called Shinkansen, was inaugurated in Japan in 1964. The train circulated at a cruise speed of 210km/h between Tokyo and Osaka. Since then, a systematic growth of the high-speed network has begun. The continuing development of vehicles and infrastructures has resulted in increased speed. The world speed record is attributed to the magnetic-levitation Maglev Train (581km/h in 2003 in Japan). This technology avoids the wheel/rail contact, which provides higher speeds while consuming less energy, but the very high cost makes them prohibitive to implement in existing rail networks. The speed record for the conventional wheeled train in test operations is held by TGV France (574.8 km/h in 2007). With increasing speed dynamic effects become more important. Some of the consequences of excessive vibrations on the track and foundation soils are: aggravation of the wear on the vehicle's wheels and of the rail route itself; instability of railway vehicles; passenger discomfort; propagation of said vibrations to neighbouring buildings, where they can cause discomfort to habitants and/or affect precision devices in industrial buildings. These issues motivate increasing effort by the scientific community on the moving load problems. Closed form analytical solutions, if obtainable, are always desirable because of their numerical efficiency and physical insight into the problem.

The chapter is organized in the following way: three important aspects that one should be aware of before starting analyses in this field are described in Section 2; governing equations are developed in a very general form in Section 3; detailed analysis of vibration modes and modal co-ordinates determination is presented in Section 4; additional issues are discussed in Section5 and the chapter is concluded in Section 6.

# 2 Three introductory issues

## 2.1 Standard finite elements

It has been proven in [10] that standard finite elements induce an error in natural frequencies that is a consequence of polynomial shape functions. This error is invariant if normalized by the total number of degrees of freedom increased by one and aggravates with the polynomial degree. Our concern is on transversal vibrations, but for the sake of simplicity, the following explanation pertains to longitudinal vibrations.

Let longitudinal vibrations of an elastic rod fixed on both ends be assumed. The stiffness and consistent mass matrices for an element of unitary axial stiffness ($EA$=1) and unitary mass per length ($\mu$=1), for linear and quadratic shape functions, can be obtained by exact integration:

$$\mathbf{K}_{p=1} = \frac{1}{h}\begin{bmatrix} 1 & -1 \\ -1 & 1 \end{bmatrix}, \ \mathbf{K}_{p=2} = \frac{1}{3h}\begin{bmatrix} 7 & -8 & 1 \\ -8 & 16 & -8 \\ 1 & -8 & 7 \end{bmatrix}, \tag{1}$$

$$\mathbf{M}_{p=1} = \frac{h}{6}\begin{bmatrix} 2 & 1 \\ 1 & 2 \end{bmatrix}, \ \mathbf{M}_{p=2} = \frac{h}{30}\begin{bmatrix} 4 & 2 & -1 \\ 2 & 16 & 2 \\ -1 & 2 & 4 \end{bmatrix}, \tag{2}$$

where $h$ designates the element length and $p$ the polynomial degree. A typical equation for an interior node of a unit length rod ($L$=1) for $p$=1 reads as:

$$\frac{1}{h}\left(\phi_{n-1} - 2\phi_n + \phi_{n+1}\right) + \omega_h^2 \frac{h}{6}\left(\phi_{n-1} + 4\phi_n + \phi_{n+1}\right) = 0, \quad n = 1,\ldots,N\,. \tag{3}$$

where $N$ is the total number of interior nodes, which is equal to the number of modes. The element length is therefore $h$=1/($N$+1). $\phi_n$ stands for a discrete value of the vibration mode and $\omega_h$ is the numerical value of the natural frequency. The boundary conditions dictate that $\phi_0 = \phi_{N+1} = 0$. This set of equations allow for analytical resolution in the form of:

$$\omega_{h,j} = \frac{1}{h}\sqrt{\frac{6\left(1-\cos\left(\omega_j h\right)\right)}{2+\cos\left(\omega_j h\right)}}, \quad j = 1,\ldots,N\,, \tag{4}$$

where $\omega_j = j\pi$ is the analytical frequency value. A plot of points $\left[\frac{j}{N+1}, \frac{\omega_{h,j}}{\omega_j}\right]$, $j$=1…$N$, is invariant with respect to $N$.

For $p$=2 the typical equation for an interior node (after condensation of mid-node degrees of freedom) is:

$$\begin{aligned} &\frac{1}{3h\left(10-\omega_h^2 h^2\right)}\left(\left(30+2\omega_h^2 h^2\right)\left(\phi_{n-1}+\phi_{n+1}\right) + \left(-60+16\omega_h^2 h^2\right)\phi_n\right) \\ &+ \omega_h^2 \frac{h}{120\left(10-\omega_h^2 h^2\right)}\left(5\omega_h^2 h^2\left(\phi_{n-1}+\phi_{n+1}\right) + \left(400-30\omega_h^2 h^2\right)\phi_n\right) = 0, \quad n = 1,\ldots,\tilde{N} \end{aligned} \tag{5}$$

where $\tilde{N}$ is the number of interior nodes (except for mid-nodes). In this case, the total number of natural frequencies corresponds to the total number of nodes, which is $N = 2\tilde{N}+1$. The element length is $h = 1/\left(\tilde{N}+1\right)$ and boundary conditions are the same as before ($\phi_0 = \phi_{N+1} = 0$). This set of equations has an analytical solution. Two values are obtained, corresponding to the acoustical and optical branches:

$$\omega_{h,j}^{acs} = \frac{2}{h}\sqrt{\frac{13+2\cos\left(\omega_j h\right) - \sqrt{124+112\cos\left(\omega_j h\right) - 11\cos^2\left(\omega_j h\right)}}{3-\cos\left(\omega_j h\right)}}, \quad j = 1,\ldots,N\,, \tag{6}$$

$$\omega_{h,j}^{opt} = \frac{2}{h}\sqrt{\frac{13+2\cos\left(\omega_j h\right) + \sqrt{124+112\cos\left(\omega_j h\right) - 11\cos^2\left(\omega_j h\right)}}{3-\cos\left(\omega_j h\right)}}, \quad j = 1,\ldots,N\,. \tag{7}$$

These numerical values are symmetrical around the middle value and the singularity point ($\omega_{h,\tilde{N}+1}^{acs} = \sqrt{10}/h = \sqrt{10}/\left(\tilde{N}+1\right)$), respectively. A plot of points $\left[\frac{j}{N+1}, \frac{\omega_{h,j}}{\omega_j}\right]$, j=1…*N*, is again invariant with respect to *N*. Results are quite different when lumped mass matrix is implemented. Values are summarized in Figure 1.

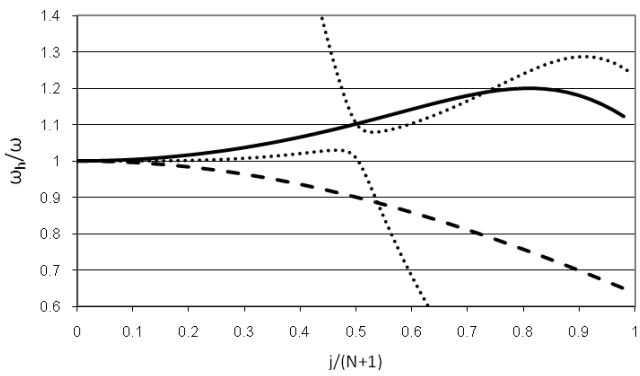


Figure 1: Ratio between the numerical and analytical values of natural frequencies: linear elements, consistent mass (solid black line), linear elements, lumped mass (dashed black lines) and quadratic elements, consistent mass (left and right dotted black lines stand for acoustical and optical branches, respectively).

It is seen in Figure 1 that the error for higher frequencies is quite large and can reach 30%. Nevertheless, if the number of degrees of freedom is at least twice the number of significant frequencies for a particular problem, the error can be kept within a reasonable value. In theory, this error could be avoided by implementation of exact shape functions. It will be seen in the next section that these functions raise several numerical issues.

## 2.2 Exact shape functions

An implementation of exact shape functions of distributed mass elements in dynamic analyses is problematical because of the presence of hyperbolic functions, which require: (i) evaluations with a high number of digits precision and (ii) capacity to deal with very large/small numbers. One can verify that 709 is the largest integer exponent that can be used in Matlab software [11] for evaluation of $e^{709}$. On the other hand Maple [12] and similar software can work easily with very large and small numbers, and adapt the number of digits precision to an arbitrary value, regardless of hardware and operating system's specifications. The limitation to double precision can induce unexpected errors, which are very hard to discover. The following example should clarify the problem. Let a cantilever clamped at the left end be assumed. In the Euler-Bernoulli (E-B) formulation, its characteristic equation is given by $1+\cos\lambda\cosh\lambda = 0$ ([10]), where $\lambda/L$ is the wave number and $L$ is the cantilever length. The natural undamped $j$-th mode shape $w_j$ reads as:

$$w_j(x) = \sin\left(\frac{\lambda_j}{L}x\right) - \frac{\sin(\lambda_j)+\sinh(\lambda_j)}{\cos(\lambda_j)+\cosh(\lambda_j)}\cos\left(\frac{\lambda_j}{L}x\right)$$
$$-\sinh\left(\frac{\lambda_j}{L}x\right) + \frac{\sin(\lambda_j)+\sinh(\lambda_j)}{\cos(\lambda_j)+\cosh(\lambda_j)}\cosh\left(\frac{\lambda_j}{L}x\right), \tag{8}$$

from which the displacement value at the free (right) end is

$$w_j(L) = \frac{2\sin\lambda_j \sinh\lambda_j}{\sinh\lambda_j - \sin\lambda_j}. \tag{9}$$

It is possible to write Equation (8) in the following form:

$$w_j(x) = \frac{1}{\sin\lambda_j - \sinh\lambda_j}\left(-\sin(\lambda_j)\sinh\left(\frac{\lambda_j}{L}x\right) - \sinh(\lambda_j)\sin\left(\frac{\lambda_j}{L}x\right)\right.$$
$$\left.+\cos\left(\frac{\lambda_j}{L}x-\lambda_j\right) - \cosh\left(\frac{\lambda_j}{L}x-\lambda_j\right) - \cos(\lambda_j)\cosh\left(\frac{\lambda_j}{L}x\right) + \cosh(\lambda_j)\cos\left(\frac{\lambda_j}{L}x\right)\right). \tag{10}$$

| | $\lambda$ | Eq.(8)100 | Eq.(10)100 | Eq.(9)100 | Eq.(8)20 | Eq.(10)20 | Eq.(9)20 |
|---|---|---|---|---|---|---|---|
| m1 | 1.87510 | 2.72444 | 2.72444 | 2.72444 | 2.72444 | 2.72444 | 2.72444 |
| m2 | 4.69409 | -1.96374 | -1.96374 | -1.96374 | -1.96374 | -1.96374 | -1.96374 |
| m3 | 7.85476 | 2.00155 | 2.00155 | 2.00155 | 2.00155 | 2.00155 | 2.00155 |
| m4 | 10.99554 | -1.99993 | -1.99993 | -1.99993 | -1.99993 | -1.99993 | -1.99993 |
| m5 | 14.13717 | 2.00000 | 2.00000 | 2.00000 | 2.00000 | 2.00000 | 2.00000 |
| m6 | 17.27876 | -2.00000 | -2.00000 | -2.00000 | -2.00000 | -2.00000 | -2.00000 |
| m7 | 20.42035 | 2.00000 | 2.00000 | 2.00000 | 2.00000 | 2.00000 | 2.00000 |
| m8 | 23.56194 | -2.00000 | -2.00000 | -2.00000 | -2.00000 | -2.00000 | -2.00000 |
| m9 | 26.70354 | 2.00000 | 2.00000 | 2.00000 | 2.00000 | 2.00000 | 2.00000 |
| m10 | 29.84513 | -2.00000 | -2.00000 | -2.00000 | -2.00000 | -2.00000 | -2.00000 |
| m11 | 32.98672 | 2.00000 | 2.00000 | 2.00000 | 2.00000 | 2.00000 | 2.00000 |
| m12 | 36.12832 | -2.00000 | -2.00000 | -2.00000 | -2.00000 | -2.00000 | -2.00000 |
| m13 | 39.26991 | 2.00000 | 2.00000 | 2.00000 | 1.99800 | 2.00000 | 2.00000 |
| m14 | 42.41150 | -2.00000 | -2.00000 | -2.00000 | -2.00000 | -2.00000 | -2.00000 |
| m15 | 45.55309 | 2.00000 | 2.00000 | 2.00000 | 1.00000 | 2.00000 | 2.00000 |
| m16 | 48.69469 | -2.00000 | -2.00000 | -2.00000 | 0.00000 | -2.00000 | -2.00000 |
| m17 | 51.83628 | 2.00000 | 2.00000 | 2.00000 | 0.00000 | 2.00000 | 2.00000 |
| m18 | 54.97787 | -2.00000 | -2.00000 | -2.00000 | 0.00000 | -2.00000 | -2.00000 |
| m19 | 58.11946 | 2.00000 | 2.00000 | 2.00000 | 0.00000 | 2.00000 | 2.00000 |
| m20 | 61.26106 | -2.00000 | -2.00000 | -2.00000 | 0.00000 | -2.00000 | -2.00000 |

Table 1: Deflection values at the free cantilever end

Table 1 summarizes deflection values of the first 20 modes at the free end of the cantilever calculated by the three formulas and different digits precision assigned as 100 and 20 in columns 3-5 and 6-8, respectively.

Cells with significant error are highlighted. It is seen that the original formula (8) leads to large unexpected error in double precision software. An alternative reformulation (10), avoiding subtraction of very large/small numbers or using a higher number of digits precision must be implemented. Equation (10) solves this particular problem. An alternative mode shape for a generic beam is given in [13].

Natural frequencies search has no simple adaptation avoiding very large/small numbers. One may object that beam structures usually do not require many mode shapes to achieve acceptable results. However, beams on elastic foundation exhibit deflection shapes that are more accentuated, requiring the superposition of many modes to represent them correctly. This is shown in the following example. Two standard European rails UIC60 of $L$=100m model the cantilever (properties are summarized in Table 2). An axle force of $P$=200kN travels at a speed of $v$=50m/s from the clamped to the free end. The elastic foundation is characterized by the Winkler constant $k$=1MN/m$^2$. Deflection shapes at t=0.5s (when the force is distant 25m from the clamped end) are shown in Figure 2. The results are for the superposition of the first $n$ modes (in Figure 2a, $n$=1,2,..,8; in Figure 2b, $n$=49,50). It is seen that 50 mode shapes are necessary for sufficiently accurate results.

| Property | Beam (2 UIC60) |
|---|---|
| Young's modulus $E$ (GPa) | 210 |
| Poisson's ratio $\nu$ | 0.3 |
| Density $\rho$ (kg/m$^3$) | 7800 |
| Transversal cross-section area $A$ (m$^2$) | $153.68 \cdot 10^{-4}$ |
| Geometrical moment of inertia $I$ (m$^4$) | $6110 \cdot 10^{-8}$ |
| Bending stiffness $EI$ (MNm$^2$) | 12.831 |
| Mass per unit length $\mu$ (kg/m) | 119.8704 |

Table 2: Characteristics of 2UIC60 rails

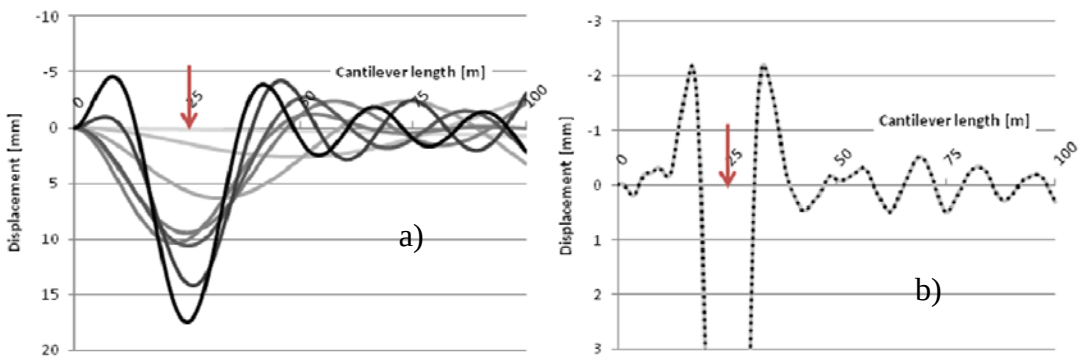


Figure 2: Cantilever on elastic foundation: a) superposition for the fist $n$ modes ($n$=1,2,...,8 from lighter to darker grey solid lines); b) for the first 49 (grey solid line) and 50 modes (black dotted line)

The same test is presented in Figure 3, but the cantilever is considered without the elastic foundation and the moving force is reduced to $P$=1kN in order to keep the displacement values within the range of validity of the linear theory.

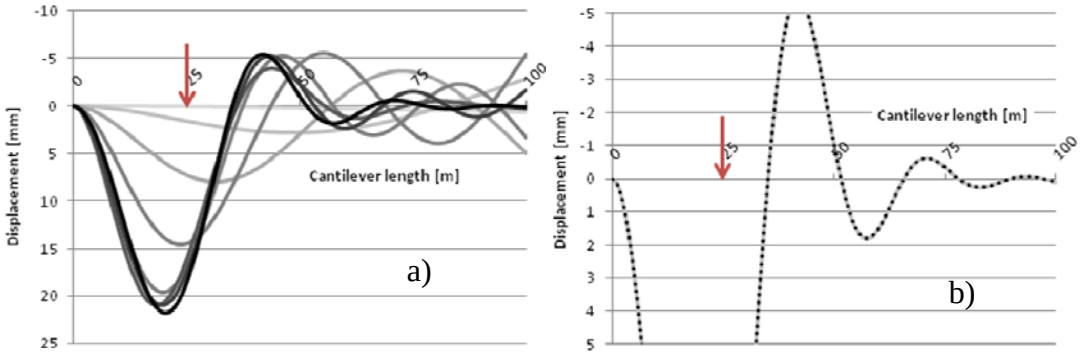


Figure 3: Cantilever without elastic foundation: a) superposition for the fist *n* modes (*n*=1,2,...,8 from lighter to darker grey solid lines); b) for the first 8 (grey solid line) and 9 modes (black dotted line)

## 2.3 Results obtained by a standard finite element software

Let the error reported in Section 2.1 be exemplified on transversal vibrations. It is necessary to point out that transversal vibrations are fundamentally different from longitudinal ones, because in higher frequencies, the effect of the shear deformation and the rotary inertia is significant even on thin beams. Commercial software is protected against inappropriate usage: for instance, in ANSYS, the effect of the rotary inertia cannot be deactivated, while the shear deformation is optional. Thus, it is not correct to evaluate the error of higher frequency values obtained by the E-B formulation. The numerical error will be analysed on a homogeneous simply supported beam because, in this case, the wave number is $\lambda_j/L=j\pi/L$ and the natural frequencies can be expressed analytically for: the E-B, the Timoshenko (T), the Timoshenko-Rayleigh (T-R) and the Rayleigh (R) theory in Equations (11-14).

$$\omega_j^2=\left(\frac{j\pi}{L}\right)^4\frac{EI}{\mu}+\frac{k}{\mu}, \tag{11}$$

$$\omega_j^2=\left(\left(\frac{j\pi}{L}\right)^4\frac{EI}{\mu}+\left(\frac{j\pi}{L}\right)^2\frac{EI}{\mu G\tilde{A}}+\frac{k}{\mu}\right)\left(1+\left(\frac{j\pi}{L}\right)^2\frac{EI}{G\tilde{A}}\right)^{-1} \tag{12}$$

$$\begin{aligned}\omega_j^2=\frac{G\tilde{A}}{2\mu r^2}\Bigg\{&1+\frac{kr^2}{G\tilde{A}}+\left(\frac{j\pi}{L}\right)^2\left(\frac{EI}{G\tilde{A}}+r^2\right)-\Bigg(\left(1-\frac{kr^2}{G\tilde{A}}\right)^2\\&-2\frac{kr^2}{G\tilde{A}}\left(\frac{j\pi}{L}\right)^2\left(\frac{EI}{G\tilde{A}}-r^2\right)+2\left(\frac{j\pi}{L}\right)^2\left(\frac{EI}{G\tilde{A}}+r^2\right)+\left(\frac{j\pi}{L}\right)^4\left(\frac{EI}{G\tilde{A}}-r^2\right)^2\Bigg)^{1/2}\Bigg\},\end{aligned} \tag{13}$$

$$\omega_j^2=\left(\left(\frac{j\pi}{L}\right)^4\frac{EI}{\mu}+\frac{k}{\mu}\right)\left(1+\left(\frac{j\pi}{L}\right)^2 r^2\right)^{-1}, \tag{14}$$

where $G$ is the shear modulus, $\tilde{A}$ is the reduced transversal cross-section area by the Timoshenko shear coefficient and $r$ is the radius of gyration. In the numerical test, two standard European rails UIC60 with $L$=100m model the simply supported beam. Their properties are summarized in Tables 2 and 3.

| Property | Beam (2 UIC60) |
|---|---|
| Coefficient of area reduction | 0.41 |
| Radius of gyration $r$ (m) | 0.063 |
| Shear stiffness $G\tilde{A}$ (MN) | 508.92 |

Table 3: Additional characteristics of 2UIC60 rails.

The beam is discretized into 250, 500, 1000 and 5000 elements and the elastic foundation is omitted. Numerical values of the first 250 and 500 natural frequencies are extracted by ANSYS software by the Block Lanczos extraction method and the consistent mass matrix, and by the preconditioned conjugate gradient (PCG) Lanczos extraction method and the lumped mass matrix. Results are summarized in Figure 4. Only the results for the first two discretizations cover the full horizontal axis. It is seen that the invariant property is maintained in Figure 4a), but separation into acoustical and optical branches is not verified. The error is much lower than predicted in [10]. There is, however, a very large error in fundamental and higher frequencies when the PCG Lanczos extraction method and lumped mass matrix are used. It reaches 17% in the fundamental value and 40% in the 500-th value for a discretization into 5000 elements. $\mu$

For an E-B beam on an elastic foundation, Equation (11) indicates that the square of the fundamental frequency is limited by $\omega_{\min}^2 = k/\mu$. This is, however, not true in others theories. For example, in the R beam, if the condition:

$$\left(\frac{j\pi}{L}\right)^4 EIr^2 + 2\left(\frac{j\pi}{L}\right)^2 EI - kr^2 \geq 0 \tag{15}$$

is not verified, then the lowest frequency is less than the square root of $k/\mu$ and it is not achieved for $j$=1. Considering Equation (14) as a function of $j$, the extreme values of $j$ and $\omega^2$ are:

$$j_{ex} = \frac{L}{\pi r}\sqrt{-1+\sqrt{1+\frac{kr^4}{EI}}}\ ,\ \omega_{\min}^2 = \frac{2EI}{\mu r^4}\left(\sqrt{1+\frac{kr^4}{EI}}-1\right). \tag{16}$$

$j_{ex}$ equals the real root of Equation (15). The closest integer to $j_{ex}$ designates the mode with the lowest frequency. In the case study considered, using a foundation stiffness of $k$=100MN/m$^2$, the order of vibration modes with respect to $j$ is 4, 3, 5, 2, 1, 6, …., as shown in Figure 5. Therefore, the modes appear in a different order than one would expect. $\omega_{\min}^2$=834209.61s$^{-2}$, $k/\mu$=834234s$^{-2}$ and frequencies of modes 4, 3, 5, 2, and 1 lie between these two values: $\omega_4^2$=834208.62s$^{-2}$ and $\omega_1^2$=834231s$^{-2}$.

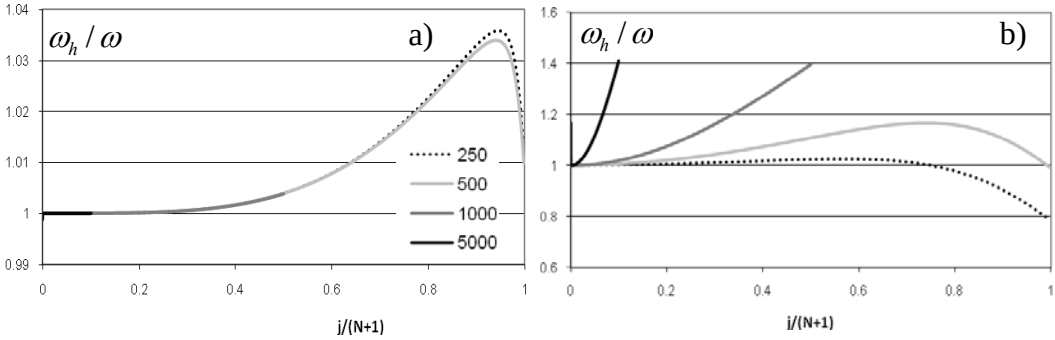


Figure 4: Error in natural frequencies: a) the Block Lanczos extraction method and the consistent mass matrix; b) the PCG Lanczos extraction method and the lumped mass matrix (the number in the legend expresses the number of elements).

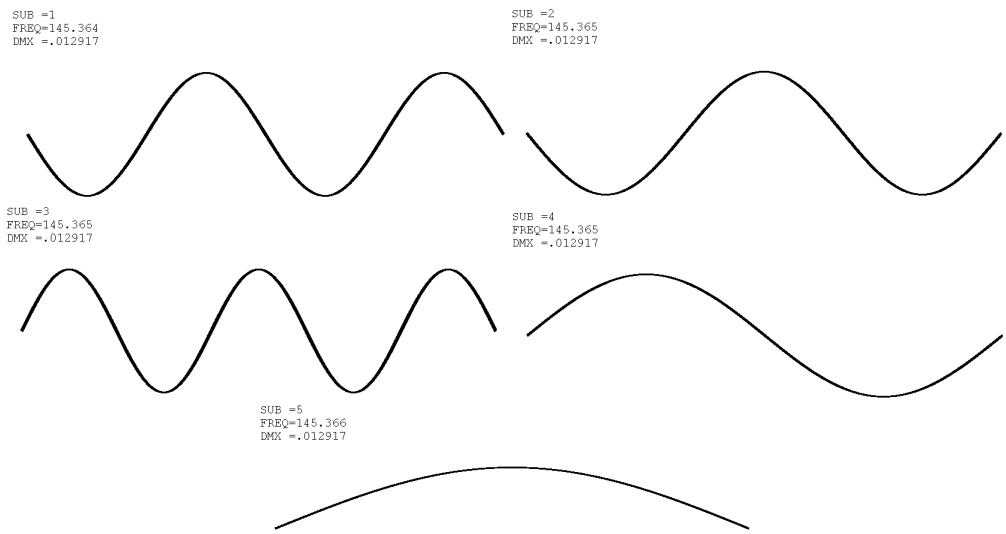


Figure 5: Modes disorder in R beam when Equation (15) is not verified.

# 3 Governing equations

## 3.1 Soil parameters

When simplified models of railways tracks are under consideration, it is necessary to substitute the effect of the underlying soil. The concern is not on the wave propagation inside the soil, but merely on the deformation properties on the surface. Deformation properties of the soil at the contact with the beam structure can be described by two frequency dependent parameters: $k(\omega)$ (Winkler model) and $k_p(\omega)$ (Filonenko–Borodich, Pasternak or Hetenyi models), that are capable of handling geometric damping. Often static values of these parameters are used in calculation models, removing the frequency dependence and thus the geometric damping.

If a harmonic motion inducing only transversal displacements is assumed, then the deflection $w$ varies inside the soil according to a function $f(z)$ and $w(x,y,z,t)=w(x,y,t)\, f(z)$, where $w(x,y,t)$ equals the deflection of the beam/soil contact

point. It holds $f(0)=1$ and $f(H)=0$, where $H$ is the so-called active depth, *i.e.* the depth of the deformable soil. In the static case the function $f(z)$ is usually linear, but in the dynamic case, its shape is frequency dependent and must be determined from the dynamic equilibrium in the vertical direction:

$$\frac{\partial \sigma_z}{\partial z} + \frac{\partial \tau_{xz}}{\partial x} + \frac{\partial \tau_{yz}}{\partial y} = \rho \frac{\partial^2 w}{\partial t^2}, \tag{17}$$

where $\sigma$ and $\tau$ stand for normal and tangential stress components, respectively. The components of the deformation tensor are given by:

$$\varepsilon_z = w(x,y,t)\frac{\mathrm{d}f(z)}{\mathrm{d}z},\ \gamma_{xz} = \frac{\partial w(x,y,t)}{\partial x} f(z),\ \gamma_{yz} = \frac{\partial w(x,y,t)}{\partial y} f(z), \tag{18}$$

where $\varepsilon$ and $\gamma$ stand for the extension and engineering distortion, respectively. Therefore, the stress components can be expressed as:

$$\sigma_z = E^{oed} w(x,y,t)\frac{\mathrm{d}f(z)}{\mathrm{d}z},\ \tau_{xz} = G\frac{\partial w(x,y,t)}{\partial x} f(z),\ \tau_{yz} = G\frac{\partial w(x,y,t)}{\partial y} f(z), \tag{19}$$

where the oedometer modulus $E^{oed}$ is given by

$$E^{oed} = E(1-\nu)/((1+\nu)(1-2\nu)). \tag{20}$$

Assuming harmonic vibrations and neglecting the shear stress derivatives, the differential equation for the function $f(z)$ reads as:

$$\frac{\mathrm{d}^2}{\mathrm{d}z^2} f(z) + \lambda^2 f(z) = 0, \tag{21}$$

where the wave number $\lambda$ is given by:

$$\lambda = \sqrt{\frac{\omega}{v_p}} = \sqrt[4]{\frac{\omega^2 \rho}{E^{oed}}}, \tag{22}$$

and $v_p$ is the velocity of the pressure waves. The solution of Equation (21) is:

$$f(z) = \cos \lambda z - \mathrm{cotg}\lambda H \sin \lambda z. \tag{23}$$

The total energy (both potential and kinetic) of the soil can be expressed as:

$$\begin{aligned} U &= \frac{1}{2}\int_{\Omega}\left\{\int_0^H \left( E^{oed}\left(\frac{\mathrm{d}f}{\mathrm{d}z}\right)^2 w^2 + Gf^2\left(\left(\frac{\partial w}{\partial x}\right)^2 + \left(\frac{\partial w}{\partial y}\right)^2\right) - \omega^2 \rho f^2 w^2 \right)\mathrm{d}z\right\}\mathrm{d}\Omega \\ &= \frac{1}{2}\int_{\Omega}\left( kw^2 + k_p\left(\left(\frac{\partial w}{\partial x}\right)^2 + \left(\frac{\partial w}{\partial y}\right)^2\right)\right)\mathrm{d}\Omega. \end{aligned} \tag{24}$$

If a sufficiently extensive area $\Omega$ is selected, the energy beyond this region can be neglected. In this formulation, the energy attributed to the Pasternak modulus in fact corresponds to the energy of distributed rotational springs. It follows:

$$k(\omega)=\int_0^H E^{oed}\left(\left(\frac{\mathrm{d}f}{\mathrm{d}z}\right)^2-(\lambda f)^2\right)dz=\frac{E^{oed}}{H}\lambda H\frac{\cos\lambda H}{\sin\lambda H}, \tag{25}$$

$$k_p(\omega)=\int_0^H Gf^2dz=\frac{1}{2}GH\left(\frac{\lambda H-\sin\lambda H\cos\lambda H}{\lambda H\sin^2\lambda H}\right) \tag{26}$$

and the vertical stress (the reaction pressure of the soil) at the contact is given by:

$$p_s=kw-k_p\left(\frac{\partial^2 w}{\partial x^2}+\frac{\partial^2 w}{\partial y^2}\right) \tag{27}$$

If $\lambda H$ tends to zero, static values of the Winkler and Pasternak parameters are obtained: $k=E^{oed}/H$ and $k_p=GH/3$. It is necessary to realize that, by adopting static values, the frequency dependence, the geometrical damping and the soil mass will be disregarded. Nevertheless, this is a common approach and will be adopted here.

Regarding the soil damping, the most correct option would be to assume hysteretic damping by elastic soil constants in the form of complex numbers. To simplify matters, viscous damping is usually implemented. In summary, the effect of the viscoelastic foundation can be represented by the soil pressure, which for beam structures takes the following form:

$$p_s=kw-k_p\frac{\partial^2 w}{\partial x^2}+c\frac{\partial w}{\partial t}-c_p\frac{\partial^3 w}{\partial x^2\partial t}. \tag{28}$$

Here $c$ and $c_p$ are distributed damping coefficients of the Winkler and Pasternak-like foundation. The Pasternak contribution is usually omitted, but there is no review work summarizing the importance of this term in railway applications, so far.

## 3.2 Governing equations

Let a uniform motion of a time dependent load along a finite horizontal beam on a viscoelastic foundation be assumed. The foundation includes both the Winkler and Pasternak viscoelastic contributions, as described in the previous section. The beam is composed of $b$ sub-domains. Within each sub-domain the beam is homogeneous, with a uniform cross section made of a linear elastic material and damping proportional to the velocity of vibration. There are $b$-1 points common to two sub-domains and two boundary nodes. Their coordinates are $x_1=0$, $x_2$,.., $x_{b+1}=L$. In all of them, localized springs, dampers and masses can be placed. The length of each sub-domain is given by $L_n=x_{n+1}-x_n$. To keep the following deductions relatively simple, prescribed displacements and/or rotations, applied concentrated forces and/or moments and internal hinges/transversal slidings are not taken into account. The load inertia is neglected at this point. Its effect is discussed in Section 5.

In Figure 6, a finite simply supported beam composed of two sub-domains with concentrated mass at the common point is shown. $P(t)$ stands for the moving force, $v$ is its constant velocity, $x$ and $w$ are the spatial coordinate and vertical deflection. The deflection is assumed positive when oriented downward and is measured from the

equilibrium position, when the beam is only loaded with its own weight. At zero time ($t$=0), the load is located at the origin of the spatial coordinate $x$.

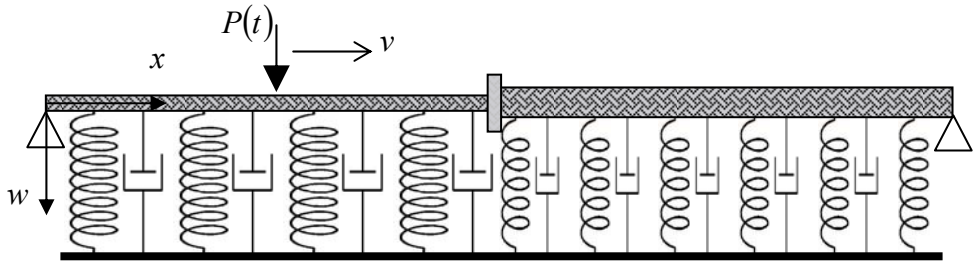


Figure 6: Simply supported beam on foundation composed of two sub-domains.

The governing equations for transversal vibrations induced by the moving force can be conveniently derived by the Hamilton principle, see *e.g.* [15] for similar development. The formulation presented is for conservative forces, so the damping influence must be included into the equations derived by analogy. For the sake of simplicity, the functional dependency *(x,t)* is written only when a particular node coordinate $x_n$ is used. The potential energy $U$ of the beam sub-domains on an elastic foundation with shear contribution governed by Pasternak coefficient $k_p$, and $U^c$ of the concentrated springs, read as:

$$U=\sum_{n=1}^{b}\frac{1}{2}\int_{x=x_n}^{x_n+L_n}\left(EI_n\left(\frac{\partial\psi_n}{\partial x}\right)^2+G\tilde{A}_n\left(\frac{\partial w_n}{\partial x}-\psi_n\right)^2+N_n\left(\frac{\partial w_n}{\partial x}\right)^2\right.$$
$$\left.+k_n w_n^2+k_{p,n}\left(\frac{\partial w_n}{\partial x}\right)^2-2pw_n\right)\mathrm{d}x, \tag{29}$$

$$U^c=\sum_{n=1}^{b+1}\frac{1}{2}\left(k_{L,n}w^2(x_n)+k_{R,n}\psi^2(x_n)\right), \tag{30}$$

where $k_{L,n}$, $k_{R,n}$, are stiffness and damping coefficients of the concentrated linear and rotational springs and dampers. $N_n$ is the axial force, assumed positive as traction, $\psi_n(x,t)$ is the bending rotation and $p(x,t)$ is a general distributed transversal external load. The kinetic energy $T$ of the beam sub-domains and $T^c$ of the concentrated masses are:

$$T=\sum_{n=1}^{b}\frac{1}{2}\int_{x=x_n}^{x_n+L_n}\left(\rho_n I_n\left(\frac{\partial\psi_n}{\partial t}\right)^2+\rho_n A_n\left(\frac{\partial w_n}{\partial t}\right)^2\right)dx\,, \tag{31}$$

$$T^c=\sum_{n=1}^{b+1}\frac{1}{2}\left(J_n\left(\frac{\partial\psi(x_n)}{\partial t}\right)^2+m_n\left(\frac{\partial w(x_n)}{\partial t}\right)^2\right), \tag{32}$$

where $m_n$ and $J_n$ are the mass and mass moment of inertia of the concentrated masses. Within sub-domains it is convenient to substitute $\rho_n I_n$ by $\mu_n r_n^2$.

It holds, for the dynamic equilibrium:

$$\delta\int_{t=t_1}^{t_2}\left(U+U^c-T-T^c\right)dt=0\,, \tag{33}$$

where $\delta$ designates variation. By variation of the terms in the potential energy, one obtains:

$$\begin{aligned}\delta U=\sum_{n=1}^{b}\int_{x=x_n}^{x_n+L_n}\Bigg(&EI_n\frac{\partial\psi_n}{\partial x}\delta\left(\frac{\partial\psi_n}{\partial x}\right)+G\tilde{A}_n\left(\frac{\partial w_n}{\partial x}-\psi_n\right)\delta\left(\frac{\partial w_n}{\partial x}-\psi_n\right)\\&+N_n\frac{\partial w_n}{\partial x}\delta\left(\frac{\partial w_n}{\partial x}\right)+k_nw_n\delta w_n+k_{p,n}\frac{\partial w_n}{\partial x}\delta\left(\frac{\partial w_n}{\partial x}\right)-2p\delta w_n\Bigg)\mathrm{d}x,\end{aligned} \tag{34}$$

$$\delta U^c=\sum_{n=1}^{b+1}\left(k_{L,n}w(x_n)\delta w(x_n)+k_{R,n}\psi(x_n)\delta\psi(x_n)\right). \tag{35}$$

Exchanging the order of the variation and the derivate and carrying out the integration by parts (the beam characteristics are constant within each sub-domain):

$$\begin{aligned}\delta U=&\sum_{n=1}^{b}\left[EI_n\frac{\partial\psi_n}{\partial x}\delta\psi_n+\left(k_{p,n}\frac{\partial w_n}{\partial x}+N_n\frac{\partial w_n}{\partial x}+G\tilde{A}_n\left(\frac{\partial w_n}{\partial x}-\psi_n\right)\right)\delta w_n\right]_{x=x_n}^{x_n+L_n}\\&+\sum_{n=1}^{b}\int_{x=x_n}^{x_n+L_n}\Bigg(\left(-EI_n\frac{\partial^2\psi_n}{\partial x^2}-G\tilde{A}_n\left(\frac{\partial w_n}{\partial x}-\psi_n\right)\right)\delta\psi_n+\Bigg(-N_n\frac{\partial^2 w_n}{\partial x^2}\\&-k_{p,n}\frac{\partial^2 w_n}{\partial x^2}-G\tilde{A}_n\left(\frac{\partial^2 w_n}{\partial x^2}-\frac{\partial\psi_n}{\partial x}\right)+k_nw_n-p\Bigg)\delta w_n\Bigg)\mathrm{d}x.\end{aligned} \tag{36}$$

Similarly, for the kinetic energy:

$$\delta T=\sum_{n=1}^{b}\int_{x=x_n}^{x_n+L_n}\left(\rho_nI_n\frac{\partial\psi_n}{\partial t}\delta\left(\frac{\partial\psi_n}{\partial t}\right)+\rho_nA_n\frac{\partial w_n}{\partial t}\delta\left(\frac{\partial w_n}{\partial t}\right)\right)dx\,, \tag{37}$$

$$\delta T^c=\sum_{n=1}^{b+1}\left(J_n\frac{\partial\psi(x_n)}{\partial t}\delta\left(\frac{\partial\psi(x_n)}{\partial t}\right)+m_n\frac{\partial w(x_n)}{\partial t}\delta\left(\frac{\partial w(x_n)}{\partial t}\right)\right). \tag{38}$$

The time integration must be added to carry out the integration by parts:

$$\begin{aligned}\int_{t=t_1}^{t_2}\delta\left(T+T^c\right)dt=&-\int_{t=t_1}^{t_2}\left(\int_{x=x_n}^{x_n+L_n}\left(\mu_nr_n^2\frac{\partial^2\psi_n}{\partial t^2}\delta\psi_n+\mu_n\frac{\partial^2 w_n}{\partial t^2}\delta w_n\right)dx\right)dt\\&-\int_{t=t_1}^{t_2}\left(\sum_{n=1}^{b+1}\left(J_n\frac{\partial^2\psi(x_n)}{\partial t^2}\delta\psi(x_n)+m_n\frac{\partial^2 w(x_n)}{\partial t^2}\delta w(x_n)\right)\right)dt.\end{aligned} \tag{39}$$

Employing Equation (33) and grouping the corresponding terms, two coupled governing equations (so-called equations of motion) for unknown displacement and rotation fields are obtained in each sub-domain:

$$\mu_n r_n^2 \frac{\partial^2 \psi_n}{\partial t^2} - EI_n \frac{\partial^2 \psi_n}{\partial x^2} - G\tilde{A}_n \left( \frac{\partial w_n}{\partial x} - \psi_n \right) = 0 \quad n = 1,...,b\,, \tag{40}$$

$$\begin{gathered} \mu_n \frac{\partial^2 w_n}{\partial t^2} - G\tilde{A}_n \left( \frac{\partial^2 w_n}{\partial x^2} - \frac{\partial \psi_n}{\partial x} \right) - N_n \frac{\partial^2 w_n}{\partial x^2} - k_{p,n} \frac{\partial^2 w_n}{\partial x^2} + k_n w_n \\ - c_{p,n} \frac{\partial^3 w_n}{\partial t \partial x^2} + c_n \frac{\partial w_n}{\partial t} = p, \quad n = 1,...,b, \end{gathered} \tag{41}$$

where the foundation damping terms were added by analogy with the stiffness terms. Continuity conditions in the common sub-domain nodes are the following:

$$w_{n-1}(x_n) = w_n(x_n), \quad n = 2,...,b\,, \tag{42a}$$

$$\psi_{n-1}(x_n) = \psi_n(x_n), \quad n = 2,...,b\,, \tag{42b}$$

$$\begin{gathered} \left( k_{p,n-1} \frac{\partial w_{n-1}}{\partial x} + c_{p,n-1} \frac{\partial^2 w_{n-1}}{\partial t \partial x} + N_{n-1} \frac{\partial w_{n-1}}{\partial x} + G\tilde{A}_{n-1} \left( \frac{\partial w_{n-1}}{\partial x} - \psi_{n-1} \right) \right) \Bigg|_{x=x_n} \\ - \left( k_{p,n} \frac{\partial w_n}{\partial x} + c_{p,n} \frac{\partial^2 w_n}{\partial t \partial x} + N_n \frac{\partial w_n}{\partial x} + G\tilde{A}_n \left( \frac{\partial w_n}{\partial x} - \psi_n \right) \right) \Bigg|_{x=x_n} \\ + k_{L,n} w(x_n) + c_{L,n} \frac{\partial w(x_n)}{\partial t} + m_n \frac{\partial^2 w(x_n)}{\partial t^2} = 0, \quad n = 2,...,b \end{gathered} \tag{42c}$$

$$\begin{gathered} \left( EI_{n-1} \frac{\partial \psi_{n-1}}{\partial x} \right) \Bigg|_{x=x_n} - \left( EI_n \frac{\partial \psi_n}{\partial x} \right) \Bigg|_{x=x_n} \\ + k_{R,n} \psi(x_n) + c_{R,n} \frac{\partial \psi(x_n)}{\partial t} + J_n \frac{\partial^2 \psi(x_n)}{\partial t^2} = 0, \quad n = 2,...,b \end{gathered} \tag{42d}$$

where $c_{L,n}$, $c_{R,n}$, are the damping coefficients of the concentrated linear and rotational dampers, added by analogy with localized springs. The boundary conditions are:

$$w_1(x_1) = 0 \text{ or} \tag{43a}$$

$$\begin{gathered} - \left( k_{p,1} \frac{\partial w_1}{\partial x} + c_{p,1} \frac{\partial^2 w_1}{\partial t \partial x} + N_1 \frac{\partial w_1}{\partial x} + G\tilde{A}_1 \left( \frac{\partial w_1}{\partial x} - \psi_1 \right) \right) \Bigg|_{x=x_1} \\ + k_{L,1} w(x_1) + c_{L,1} \frac{\partial w(x_1)}{\partial t} + m_1 \frac{\partial^2 w(x_1)}{\partial t^2} = 0, \end{gathered} \tag{43b}$$

$$w_b(x_b) = 0 \text{ or} \tag{43c}$$

$$\begin{gathered} \left( k_{p,b} \frac{\partial w_b}{\partial x} + c_{p,b} \frac{\partial^2 w_b}{\partial t \partial x} + N_b \frac{\partial w_b}{\partial x} + G\tilde{A}_b \left( \frac{\partial w_b}{\partial x} - \psi_b \right) \right) \Bigg|_{x=x_b}, \\ + k_{L,b} w(x_b) + c_{L,b} \frac{\partial w(x_b)}{\partial t} + m_b \frac{\partial^2 w(x_b)}{\partial t^2} = 0, \end{gathered} \tag{43d}$$

$$\psi_1(x_1) = 0 \text{ or} \tag{43e}$$

$$-\left(EI_1 \frac{\partial \psi_1}{\partial x}\right)\Bigg|_{x=x_1} + k_{R,1}\psi(x_1) + c_{R,1}\frac{\partial \psi(x_1)}{\partial t} + J_1 \frac{\partial^2 \psi(x_1)}{\partial t^2} = 0 \tag{43f}$$

$$\psi_b(x_b) = 0 \text{ or} \tag{43g}$$

$$\left(EI_b \frac{\partial \psi_b}{\partial x}\right)\Bigg|_{x=x_b} + k_{R,b}\psi(x_b) + c_{R,b}\frac{\partial \psi(x_b)}{\partial t} + J_b \frac{\partial^2 \psi(x_b)}{\partial t^2} = 0\,. \tag{43h}$$

Equations (40-41) can be uncoupled, so either of the following can be used

$$\begin{gathered} EI_n \frac{\partial^4 w_n}{\partial x^4} - \mu_n r_n^2 \frac{\partial^4 w_n}{\partial t^2 \partial x^2} + \left(1 + \frac{\mu_n r_n^2}{G\tilde{A}_n}\frac{\partial^2}{\partial t^2} - \frac{EI_n}{G\tilde{A}_n}\frac{\partial^2}{\partial x^2}\right) \\ \left(\mu_n \frac{\partial^2 w_n}{\partial t^2} - N_n \frac{\partial^2 w_n}{\partial x^2} + k_n w_n - k_{p,n}\frac{\partial^2 w_n}{\partial x^2} + c_n \frac{\partial w_n}{\partial t} - c_{p,n}\frac{\partial^3 w_n}{\partial t \partial x^2}\right) \\ = p + \frac{\mu_n r_n^2}{G\bar{A}_n}\frac{\partial^2 p}{\partial t^2} - \frac{EI_n}{G\bar{A}_n}\frac{\partial^2 p}{\partial x^2}, \quad n = 1,\ldots,b \end{gathered} \tag{44}$$

$$\begin{gathered} EI_n \frac{\partial^4 \psi_n}{\partial x^4} - \mu_n r_n^2 \frac{\partial^4 \psi_n}{\partial t^2 \partial x^2} + \left(1 + \frac{\mu_n r_n^2}{G\tilde{A}_n}\frac{\partial^2}{\partial t^2} - \frac{EI_n}{G\tilde{A}_n}\frac{\partial^2}{\partial x^2}\right) \\ \left(\mu_n \frac{\partial^2 \psi_n}{\partial t^2} - N_n \frac{\partial^2 \psi_n}{\partial x^2} + k_n \psi_n - k_{p,n}\frac{\partial^2 \psi_n}{\partial x^2} + c_n \frac{\partial \psi_n}{\partial t} - c_{p,n}\frac{\partial^3 \psi_n}{\partial t \partial x^2}\right) \\ = \frac{\partial p}{\partial x}, \quad n = 1,\ldots,b. \end{gathered} \tag{45}$$

It is seen that, except for the right hand side, Equations (44-45) are exactly the same, as expected. Similar uncoupling can be done in continuity and boundary conditions. For the complete problem definition, initial conditions must also be stated. The beam bending moment and the shear and transversal forces are:

$$M_n = -EI_n \frac{\partial \psi_n}{\partial x}, \tag{46}$$

$$V_n = G\tilde{A}_n\left(\frac{\partial w_n}{\partial x} - \psi_n\right). \tag{47}$$

$$Q_n = G\tilde{A}_n\left(\frac{\partial w_n}{\partial x} - \psi_n\right) + \left(N_n + k_{p,n}\right)\frac{\partial w_n}{\partial x} + c_{p,n}\frac{\partial^2 w_n}{\partial t \partial x}\,. \tag{48}$$

The transversal force $Q_n$ enters the nodal equilibrium in the transversal direction (Equation (42c)) and therefore it is used in the dynamic stiffness matrix assembly, therefore its values are only important in a sub-domain end nodes.

# 4 Solution

## 4.1 Solution methods

The transient behaviour of general one-dimensional distributed dynamic systems, like vibrations on beam structures induced by moving loads, are often studied by implementing the Fourier method of variable separation and assuming the existence of free harmonic vibrations, which for the R-T formulation presented above means that:

$$w(x,t) = w(x)e^{i\omega t} \text{ and } \psi(x,t) = \psi(x)e^{i\omega t}, \tag{49}$$

where $i = \sqrt{-1}$. The frequency $\omega$ of these vibrations is named as the natural frequency and it is determined from the eigenvalue problem obtained from the homogeneous governing equation (both Equations (44) or (45) can be used) by substitution of Equation (49). Natural vibration modes are independent in the sense that an excitation of one mode will never cause motion of a different mode. Then the transient response in the time domain is expressed as an infinite series of these modes, where each vibration mode (function of the spatial coordinate x) is multiplied by a generalized displacement (modal coordinate, amplitude function) that is a function of time.

This solution method is called the eigenvalues expansion, the modal expansion, the modal superposition, the modal analysis, the normal mode analysis, and so on. If the governing equations can be written in a form of a self-adjoint system, then the modal analysis is facilitated by the orthogonality relations among system eigenfunctions. As a consequence, an eigenfunction series representation of system response decouples the original equations of motion into a set of independent equations governing the unknown time-dependent generalized displacements. The convergence of the series solution is guaranteed by the completeness of system eigenfunctions. The analysis steps should follow this order strictly: find eigensolutions, establish orthogonality conditions, define normalization coefficients (modal mass) and determine modal coordinates, which can be accomplished by integral transformations (*e.g.* Laplace transformation), by implementation of the Duhamel integral or by other standard solution methods of ordinary differential equations.

Conventional modal expansion is not directly applicable to non-self-adjoint systems, because the eigenfunctions are not orthogonal. For certain non-self-adjoint distributed systems, the closed form transient response can be expressed by a series of bi-orthogonal eigenfunctions in a state space formulation. In this generalized modal analysis, the completeness of the state space eigenfunctions is often assumed without justification [20]. Augmented spatial operations are introduced in [21] to account for general external, initial and boundary disturbances.

Nevertheless, even in self-adjoint systems, modal expansion is commonly governed by undamped vibration modes, because this allows their determination within the real domain and completeness of the eigenspace is guaranteed. In that

case, uncoupling the equations of motion is only possible if the system possesses so-called Rayleigh's damping. It is important to realize that, in such a case, expansion over damped eigenmodes brings no improvement.

## 4.2 Natural frequencies and mode shapes

Let damping terms be disregarded for now. By substitution of Equation (49) into (44), it holds within each sub-domain:

$$EI_n \frac{\mathrm{d}^4 w_n}{\mathrm{d}x^4} + \mu_n r_n^2 \omega^2 \frac{\mathrm{d}^2 w_n}{\mathrm{d}x^2} + \left(1 - \frac{\mu_n r_n^2 \omega^2}{G\tilde{A}_n} - \frac{EI_n}{G\tilde{A}_n}\frac{\mathrm{d}^2}{\mathrm{d}x^2}\right)$$
$$\left(-\mu_n \omega^2 w_n - N_n \frac{\mathrm{d}^2 w_n}{\mathrm{d}x^2} + k_n w_n - k_{p,n}\frac{\mathrm{d}^2 w}{\mathrm{d}x^2}\right) = 0, \quad n = 1,\ldots,b. \tag{50}$$

Equation (50) is verified by $e^{s_n x}$, thus:

$$s_n^4 + B_n s_n^2 + D_n = 0, \quad n = 1,\ldots,b, \tag{51}$$

where

$$B_n = \frac{G\tilde{A}_n \mu_n r_n^2 \omega^2 + \left(N_n + k_{p,n}\right)\left(\mu_n r_n^2 \omega^2 - G\tilde{A}_n\right) + EI_n\left(\mu_n \omega^2 - k_n\right)}{EI_n\left(G\tilde{A}_n + N_n + k_{p,n}\right)}, \tag{52}$$

$$D_n = \frac{\left(\mu_n \omega^2 - k_n\right)\left(\mu_n r_n^2 \omega^2 - G\tilde{A}_n\right)}{EI_n\left(G\tilde{A}_n + N_n + k_{p,n}\right)}. \tag{53}$$

$s_n$ is named the wave number (compare with the previously used $\lambda/L$ in Sections 2.2 and 2.3). In most cases, the four roots of Equation (51) are either real or imaginary and can be expressed analytically as:

$$s_{n,1} = i\sqrt{\frac{B_n}{2} + \sqrt{\left(\frac{B_n}{2}\right)^2 - D_n}}\ ,\ s_{n,2} = -i\sqrt{\frac{B_n}{2} + \sqrt{\left(\frac{B_n}{2}\right)^2 - D_n}}\ , \tag{54a}$$

$$s_{n,3} = \sqrt{-\frac{B_n}{2} + \sqrt{\left(\frac{B_n}{2}\right)^2 - D_n}}\ ,\ s_{n,4} = -\sqrt{-\frac{B_n}{2} + \sqrt{\left(\frac{B_n}{2}\right)^2 - D_n}}\ . \tag{54b}$$

The general form of the mode shape within each sub-domain can be written as:

$$w_n(x) = \sum_{l=1}^{4} C_{n,l} \mathrm{e}^{s_{n,l} x}\ . \tag{55a}$$

According to particular numerical values, mode representation in purely real domain is possible in the following forms:

$$D_n < \left(\frac{B_n}{2}\right)^2 \;\&\; \sqrt{\left(\frac{B_n}{2}\right)^2 - D_n} > \left|\frac{B_n}{2}\right| \quad \Rightarrow$$
$$w_n(x) = C_{n,1}\cos(\bar{s}_{n,1}x) + C_{n,2}\sin(\bar{s}_{n,1}x) + C_{n,3}\cosh(s_{n,3}x) + C_{n,4}\sinh(s_{n,3}x) \tag{55b}$$

$$D_n \le \left(\frac{B_n}{2}\right)^2 \;\&\; \sqrt{\left(\frac{B_n}{2}\right)^2 - D_n} < \frac{B_n}{2} \quad \Rightarrow$$
$$w_n(x) = C_{n,1}\cos(\bar{s}_{n,1}x) + C_{n,2}\sin(\bar{s}_{n,1}x) + C_{n,3}\cos(\bar{s}_{n,3}x) + C_{n,4}\sin(\bar{s}_{n,3}x) \tag{55c}$$

$$D_n > \left(\frac{B_n}{2}\right)^2 \quad \Rightarrow$$
$$w_n(x) = \mathrm{e}^{\mathrm{Re}(s_{n,5})x}\left(C_{n,1}\cos(\mathrm{Im}(s_{n,5})x) + C_{n,2}\sin(\mathrm{Im}(s_{n,5})x)\right) \tag{55d}$$

The validity of Equations (55b-d) is dependent on the value of the still unknown natural frequency. Equation (55d) defines a mode shape using alternative values to those specified in Equations (54), because in this case all roots will have a real and an imaginary part. The $s_{n,5}$ value can be determined from the original roots by methods of complex analysis. It corresponds to a root with a negative real part. All four roots are located on a circle with the radius equal to $\sqrt[4]{D_n}$. Two roots with the positive real part form a non-physical solution, therefore $C_{n,3}$=$C_{n,4}$=0. Such a mode resembles the deflection shape of an infinite beam and, in our case, will affect only a small part of the corresponding sub-domain. The corresponding frequency will be below the square root of $k_n/\mu_n$, but the reasoning is different than in the case study of Section 2.3.

Since the homogeneous part of Equations (44-45) is the same, the general relation for the bending rotation can be written using the same roots and constants as:

$$\psi_n(x) = \sum_{l=1}^{4} C_{n,l}\hat{s}_{n,l}e^{s_{n,l}x} \,. \tag{56}$$

The relation between $s_{n,l}$ and $\hat{s}_{n,l}$ can be obtained by substitution into original coupled Equations (40) or (41):

$$\hat{s}_{n,l} = s_{n,l} + \frac{1}{G\tilde{A}_n s_{n,l}}\left(\left(N_n + k_{p,n}\right)s_{n,l}^2 + \mu_n\omega^2 - k_n\right) = \frac{G\tilde{A}_n s_{n,l}}{G\tilde{A}_n - EI_n s_{n,l}^2 - \mu_n r_n^2\omega^2} \,. \tag{57}$$

It is seen that it is closely related to the right-hand side of Equation (44), as expected. The bending moment and the transversal force are:

$$M_n = -EI_n\sum_{l=1}^{4} C_{n,l}\hat{s}_{n,l}s_{n,l}e^{s_{n,l}x} \,, \tag{58}$$

$$
\begin{aligned}
Q_n &= G\tilde{A}_n\left(\frac{dw_n}{dx}-\psi_n\right)+\left(N_n+k_{p,n}\right)\frac{dw_n}{dx} \\
&= G\tilde{A}_n\left(\sum_{l=1}^{4}C_{n,l}\left(s_{n,l}-\hat{s}_{n,l}\right)e^{s_{n,l}x}\right)+\left(N_n+k_{p,n}\right)\left(\sum_{l=1}^{4}C_{n,l}s_{n,l}e^{s_{n,l}x}\right),
\end{aligned}
\tag{59}
$$

which can be rewritten to:

$$
\begin{aligned}
Q_n = EI_n\Big(&\hat{s}_{n,1}\hat{s}_{n,3}\left(C_{n,1}s_{n,3}e^{s_{n,1}x}+C_{n,3}s_{n,1}e^{s_{n,3}x}\right) \\
&\hat{s}_{n,2}\hat{s}_{n,4}\left(C_{n,2}s_{n,4}e^{s_{n,2}x}+C_{n,4}s_{n,2}e^{s_{n,4}x}\right)\Big).
\end{aligned}
\tag{60}
$$

Mode shape descriptions in different sub-domains are connected by the continuity Equations (42), and by the fact that the frequency of the harmonic movement must be the same. The boundary Equations (43) must also be verified. In order to reduce the number of equations to be solved, a local dynamic stiffness matrix can be derived for a general sub-domain. The global dynamic stiffness matrix is then assembled by the direct stiffness method and localized disturbances from Equations (42-43) simply can be added. Alternatively, local disturbances can be added to modal coordinates determination, as explained in Section 4.3. Following this method, a set of homogeneous equations is obtained for unknown displacements and rotations of the sub-domains common points. The $\omega$ values ensuring the nullity of the determinant, *i.e.* the existence of a non-trivial solution, are named as the natural frequencies, $\omega_j$. Substituting $\omega=\omega_j$ back into the global matrix, unknown nodal displacements and rotations can be determined.

A quite general expression of the local dynamic stiffness matrix can be found in [16]. Here, for the sake of simplicity, the following analysis is reduced to an E-B beam on a Winkler foundation without the effect of the normal force. In such a case mode shape in most cases can be written by Equation (55b) and:

$$
\bar{s}_{n,1}=s_{n,3}=\frac{\lambda_n}{L_n}=\sqrt[4]{\frac{\mu_n\omega^2-k_n}{EI_n}}\ ,
\tag{61}
$$

that immediately allow concluding that for $\mu_n\omega^2-k_n<0$ Equation (55d) must be used and

$$
s_{n,5}=\left(-1+i\right)\sqrt[4]{\frac{k_n-\mu_n\omega^2}{4EI_n}}\ .
\tag{62}
$$

The frequency connection between sub-domains is written as:

$$
\omega=\sqrt{\frac{\lambda_1^4}{L_1^4}\frac{EI_1}{\mu_1}+\frac{k_1}{\mu_1}}=\sqrt{\frac{\lambda_2^4}{L_2^4}\frac{EI_2}{\mu_2}+\frac{k_2}{\mu_2}}=\ldots=\sqrt{\frac{\lambda_b^4}{L_b^4}\frac{EI_b}{\mu_b}+\frac{k_b}{\mu_b}}\ ,
\tag{63}
$$

which implies that the natural frequency values are limited by $\omega_{\min}^2=\left(k/\mu\right)_{\min}$. It can also be concluded that the first vibration modes excite only the softest part of the structure, while in the stronger sub-domains deflection shape is almost negligible,

described by Equation (55d). The full structure is affected by the vibration modes only after the natural frequencies overpass the square root of $(k/\mu)_{\max}$. This implies that, if there is a large difference between $(k/\mu)_{\min}$ and $(k/\mu)_{\max}$, a very high number of modes must be used in modal superposition.

The local dynamic stiffness matrix of the $n$-th sub-domain can be calculated in the following way. The degrees of freedom are represented in Figure 7a). Excitation with unit amplitude and given circular frequency $\omega$ is assumed in the direction of one of the degrees of freedom, while the other degrees of freedom are kept fixed. Figure 7b) exemplifies implementation of the first degree of freedom and orientation of the corresponding terms of the stiffness matrix.

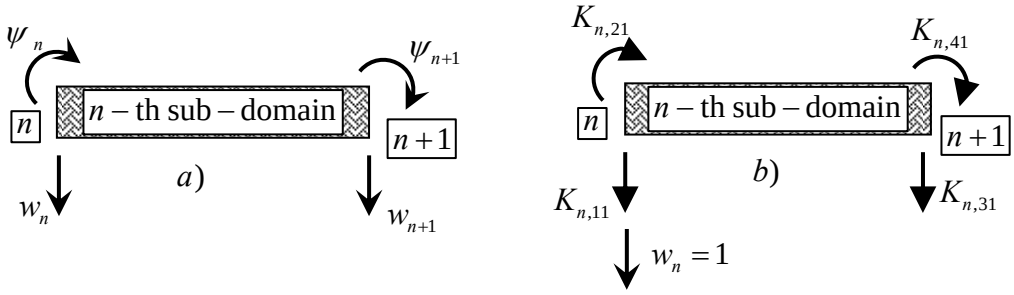


Figure 7: a) Degrees of freedom, b) construction of the local dynamic stiffness matrix of the $n$-th sub-domain.

For such an excitation, member-end generalized harmonic forces in the steady-state regime are calculated exploiting Equations (58) and (60). The procedure is repeated for the other degrees of freedom. Obviously:

$$K_{n,1m} = -Q_{n,m}(x_n),\ K_{n,2m} = M_{n,m}(x_n), \tag{64a}$$

$$K_{n,3m} = Q_{n,m}(x_{n+1}),\ K_{n,4m} = -M_{n,m}(x_{n+1}), \tag{64b}$$

where $m$ designates the order of the degree of freedom that was used for excitation. The dynamic stiffness matrix is a symmetric 4x4 matrix composed by harmonic functions with amplitudes shown below in Equation (65).

$$\begin{Bmatrix} -Q_n(x_n) \\ M_n(x_n) \\ Q_n(x_{n+1}) \\ -M_n(x_{n+1}) \end{Bmatrix} = EI_n \begin{bmatrix} F_{n,6}/L_n^3 & -F_{n,4}/L_n^2 & F_{n,5}/L_n^3 & F_{n,3}/L_n^2 \\ & F_{n,2}/L_n & -F_{n,3}/L_n^2 & F_{n,1}/L_n \\ & & F_{n,6}/L_n^3 & F_{n,4}/L_n^2 \\ symm. & & & F_{n,2}/L_n \end{bmatrix} \cdot \begin{Bmatrix} w_n \\ \psi_n \\ w_{n+1} \\ \psi_{n+1} \end{Bmatrix}, \tag{65}$$

The terms in Equation (65) make use of the following Kolousek's functions [5]:

$$F_{1,n} = -\lambda_n \frac{\sinh\lambda_n - \sin\lambda_n}{\cosh\lambda_n \cos\lambda_n - 1},\ F_{2,n} = -\lambda_n \frac{\cosh\lambda_n \sin\lambda_n - \sinh\lambda_n \cos\lambda_n}{\cosh\lambda_n \cos\lambda_n - 1},$$

$$F_{3,n} = -\lambda_n^2 \frac{\cosh\lambda_n - \cos\lambda_n}{\cosh\lambda_n \cos\lambda_n - 1},\ F_{4,n} = \lambda_n^2 \frac{\sinh\lambda_n \sin\lambda_n}{\cosh\lambda_n \cos\lambda_n - 1}, \tag{66}$$

$$F_{5,n} = \lambda_n^3 \frac{\sinh\lambda_n + \sin\lambda_n}{\cosh\lambda_n \cos\lambda_n - 1},\ F_{6,n} = -\lambda_n^3 \frac{\cosh\lambda_n \sin\lambda_n + \sinh\lambda_n \cos\lambda_n}{\cosh\lambda_n \cos\lambda_n - 1}.$$

Such a local stiffness matrix corresponds to an interior sub-domain with both ends fixed. A boundary sub-domain can be simplified by methods of degrees of freedom condensation, depending on the boundary conditions. After the global matrix has been assembled, Equation (63) can be substituted and the determinant can be expressed in terms of a single unknown, $\omega$ or $\omega^2$. Except for very simple cases, the determinant contains a quite complicated combination of trigonometric and hyperbolic functions, requiring numerical search of the roots. The determinant has many singularities coincident with all natural frequencies of each sub-domain considered separately. In order to avoid special treatment around the singularities, it is possible to solve the roots in the numerator. More details can be found in [13].

## 4.3 Relation to the infinite beam

The local dynamic stiffness matrix of a single sub-domain can be related to an infinite beam. Let semi-infinite sub-domains be considered first. In this case, only two degrees of freedom must be considered, as exemplified in Figure 8. From the roots specified in Equations (54), the negative-valued ones are used in the positive semi-infinite sub-domains to ensure vanishing of the displacements and rotations for $x$ tending to positive infinity, and *vice versa*.

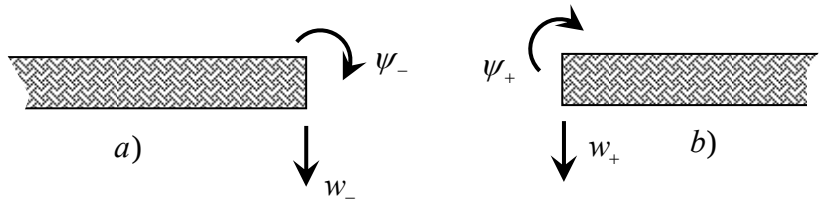


Figure 8: Degrees of freedom of semi-infinite sub-domains: a) negative, b) positive.

It yields for the positive and negative semi-infinite sub-domains:

$$\mathbf{K}_+ = \begin{bmatrix} \left(G\tilde{A} + N + k_p\right)\dfrac{\hat{s}_4 s_2 - \hat{s}_2 s_4}{\hat{s}_2 - \hat{s}_4} & \dfrac{-\left(G\tilde{A} + N + k_p\right)\left(s_2 - s_4\right) + G\tilde{A}\left(\hat{s}_2 - \hat{s}_4\right)}{\hat{s}_2 - \hat{s}_4} \\ EI\dfrac{\hat{s}_2\hat{s}_4\left(s_2 - s_4\right)}{\hat{s}_2 - \hat{s}_4} & -EI\dfrac{\hat{s}_2 s_2 - \hat{s}_4 s_4}{\hat{s}_2 - \hat{s}_4} \end{bmatrix} \tag{67a}$$

$$= \frac{EI}{\hat{s}_2 - \hat{s}_4}\begin{bmatrix} -\hat{s}_2\hat{s}_4\left(\hat{s}_2 s_2 - \hat{s}_4 s_4\right) & \hat{s}_2\hat{s}_4\left(s_2 - s_4\right) \\ \hat{s}_2\hat{s}_4\left(s_2 - s_4\right) & -\left(\hat{s}_2 s_2 - \hat{s}_4 s_4\right) \end{bmatrix},$$

$$\mathbf{K}_{-}=\begin{bmatrix}\left(G\tilde{A}+N+k_p\right)\dfrac{\hat{s}_1 s_3-\hat{s}_3 s_1}{\hat{s}_1-\hat{s}_3} & \dfrac{\left(G\tilde{A}+N+k_p\right)\left(s_1-s_3\right)-G\tilde{A}\left(\hat{s}_1-\hat{s}_3\right)}{\hat{s}_1-\hat{s}_3}\\ -EI\dfrac{\hat{s}_1\hat{s}_3\left(s_1-s_3\right)}{\hat{s}_1-\hat{s}_3} & EI\dfrac{\hat{s}_1 s_1-\hat{s}_3 s_3}{\hat{s}_1-\hat{s}_3}\end{bmatrix} \tag{67b}$$

$$=\frac{EI}{\hat{s}_1-\hat{s}_3}\begin{bmatrix}\hat{s}_1\hat{s}_3\left(\hat{s}_1 s_1-\hat{s}_3 s_3\right) & -\hat{s}_1\hat{s}_3\left(s_1-s_3\right)\\ -\hat{s}_1\hat{s}_3\left(s_1-s_3\right) & \hat{s}_1 s_1-\hat{s}_3 s_3\end{bmatrix}.$$

It can be verified simply that $\mathbf{K}=\mathbf{K}_{+}+\mathbf{K}_{-}$ is diagonal and corresponds to the action of a static load on an infinite beam. In order to account for the moving load, the governing Equations (40-41) had to be derived in the moving coordinate system [18]. Then, Equation (51) would include $s_n^3$, $s_n$ and its coefficients would have the load velocity $v$ implemented. By substitution of $v$=0, the original Equation (51) would be obtained. The full matrix **K** would be non-symmetric and $v=v_{crit}$ (the critical velocity) would ensure the nullity of its determinant. A single "mode" shape would define the deflection shape similarly to Equations (55d) and (55c) for subcritical velocities and critical velocities, respectively. Full determination of the quasi-stationary deflection shape would still require the continuity equations at the point of load application. In this case, damping inclusion would cause no problems. The same results as in [6] would be obtained, placing the concept of the dynamic stiffness matrix as a general principle for finite, semi-infinite and infinite beams.

Going back to the stiffness matrixes of the semi-infinite sub-domains (Equations (67)), one can verify that they correspond to the limit of the corresponding terms of the general fixed-fixed or fixed-free sub-domain, when their length tends to infinity. Indeed, for an E-B beam on a Winkler foundation:

$$\mathbf{K}_{+}=EI\begin{bmatrix}-\tilde{\lambda}^3(1-i) & i\tilde{\lambda}^2\\ i\tilde{\lambda}^2 & \tilde{\lambda}(1+i)\end{bmatrix},\ \mathbf{K}_{-}=EI\begin{bmatrix}-\tilde{\lambda}^3(1-i) & -i\tilde{\lambda}^2\\ -i\tilde{\lambda}^2 & \tilde{\lambda}(1+i)\end{bmatrix}, \tag{68}$$

where $s_1=i\tilde{\lambda}$, $s_3=\tilde{\lambda}$, $s_2=-i\tilde{\lambda}$, $s_4=-\tilde{\lambda}$. Then, $\mathbf{K}_{+}$ corresponds to the limit of the fixed-free (Equation (69)) and fixed-fixed sub-domain (Equation (65-66)) terms, and analogously for $\mathbf{K}_{-}$.

$$K_{11}^{fr}=-\frac{EI\lambda^3}{L^3}\frac{\cosh\lambda\sin\lambda+\sinh\lambda\cos\lambda}{\cosh\lambda\cos\lambda+1}, \tag{69a}$$

$$K_{12}^{fr}=-\frac{EI\lambda^2}{L^2}\frac{\sinh\lambda\sin\lambda}{\cosh\lambda\cos\lambda+1}, \tag{69b}$$

$$K_{22}^{fr}=-\frac{EI\lambda}{L}\frac{\cosh\lambda\sin\lambda-\sinh\lambda\cos\lambda}{\cosh\lambda\cos\lambda+1}. \tag{69c}$$

One can see that the stiffness matrix of an E-B, undamped, semi-infinite sub-domain involves complex numbers, which complicates its implementation. These stiffness matrix terms could be interpreted as localized wave-number dependent boundary

springs and dampers, but the numerical determination of natural frequencies in such cases is not simple. Semi-infinite elements can work as an absorbing boundary.

## 4.4 Forced vibrations - generalized displacement

The general solution of Equation (44) is assumed in the form of:

$$w(x,t)=\sum_{j=1}^{\infty} q_j(t) w_j(x), \tag{70}$$

where $q_j$ designates the j-th generalized displacement, but Equation (44) is not convenient for $q_j$ determination, because it has fourth order time derivatives. Generally, the state-space form of the governing equations is more adequate at this point and will be explained later on. Nevertheless, the fundamental issues are more easily explained on a simple case.

Let an E-B beam on a Winkler viscoelastic foundation, with no effect of the normal force, be considered first. Let the localized disturbances (springs, dampers and masses) be only linear. Then, the governing Equations (40-41) or (44) can be simplified as:

$$\begin{aligned} &EI(x)\frac{\partial^4 w}{\partial x^4}+\mu(x)\frac{\partial^2 w}{\partial t^2}+c(x)\frac{\partial w}{\partial t}+k(x)w \\ &+\sum_{n=1}^{b+1}\delta(x-x_n)\left(m_n\frac{\partial^2 w}{\partial t^2}+c_{L,n}\frac{\partial w}{\partial t}+k_{L,n}w\right)=p, \end{aligned} \tag{71}$$

where $\delta$ is the Dirac delta function. Here, the piece-wise constant dependence of the beam characteristics is expressed as a function of $x$, and the localized effects, formerly included in the continuity and boundary Equations (42-43), constitute an integral part of the governing Equation (71). There are two possibilities for determining generalized displacements. They are distinguished by the fact, whether the continuity and boundary conditions (42-43) are included in the natural modes determination or not. In the former case, the undamped vibration modes verify:

$$\begin{aligned} &\left(EI(x)\frac{\mathrm{d}^4}{\mathrm{d}x^4}+k(x)+\sum_{n=1}^{b+1}\delta(x-x_n)k_{L,n}\right)w_j \\ &-\omega_j^2\left(\mu(x)+\sum_{n=1}^{b+1}\delta(x-x_n)m_n\right)w_j=0, \quad \forall j, \end{aligned} \tag{72}$$

which means that if

$$\begin{aligned} &\int_{x=0}^{L} w_l\frac{\mathrm{d}^4 w_j}{\mathrm{d}x^4}\mathrm{d}x=\left[w_l\frac{\mathrm{d}^3 w_j}{\mathrm{d}x^3}\right]_0^L-\left[\frac{\mathrm{d}w_l}{\mathrm{d}x}\frac{\mathrm{d}^2 w_j}{\mathrm{d}x^2}\right]_0^L+\left[\frac{\mathrm{d}^2 w_l}{\mathrm{d}x^2}\frac{\mathrm{d}w_j}{\mathrm{d}x}\right]_0^L \\ &-\left[\frac{\mathrm{d}^3 w_l}{\mathrm{d}x^3}w_j\right]_0^L+\int_{x=0}^{L}\frac{d^4 w_l}{dx^4}w_j\mathrm{d}x=\int_{x=0}^{L}\frac{d^4 w_l}{dx^4}w_j\mathrm{d}x, \end{aligned} \tag{73}$$

the system is self-adjoint and the following two orthogonality conditions are fulfilled:

$$\int_0^L \mu(x) w_j w_l \mathrm{d}x + \sum_{n=1}^{b+1} m_n w_j(x_n) w_l(x_n) = 0, \quad \forall j \neq l\,, \tag{74a}$$

$$M_j = \int_0^L \mu(x) w_j^2 \mathrm{d}x + \sum_{n=1}^{b+1} m_n w_j^2(x_n), \quad \forall j\,, \tag{74b}$$

$$\int_0^L EI(x) \frac{\mathrm{d}^4 w_j}{\mathrm{d}x^4} w_l \mathrm{d}x + \int_0^L k(x) w_j w_l \mathrm{d}x + \sum_{n=1}^{b+1} k_{L,n} w_j(x_n) w_l(x_n) = 0, \quad \forall j \neq l, \tag{74c}$$

$$\int_0^L EI(x) \frac{\mathrm{d}^4 w_j}{\mathrm{d}x^4} w_j \mathrm{d}x + \int_0^L k(x) w_j^2 \mathrm{d}x + \sum_{n=1}^{b+1} k_{L,n} w_j^2(x_n) = S_j, \quad \forall j, \tag{74d}$$

where $M_j$ is called the modal mass, but $S_j$ usually does not have a particular designation. The terms in brackets in Equation (73) are zero, because homogeneous boundary conditions are assumed. From the positivity of the potential and kinetic energy, it follows that natural frequencies are real. By substitution of Equation (70) into Equation (71), multiplication by a mode shape function, integration over the full length structure and exploiting Equations (74):

$$S_j q_j + M_j \frac{\mathrm{d}^2 q_j}{\mathrm{d}t^2} + \int_{x=0}^L \left( c(x) + \sum_{n=1}^{b+1} \delta(x - x_n) c_{L,n} \right) \sum_{l=1}^{\infty} \frac{\mathrm{d}q_l}{\mathrm{d}t} w_l w_j \mathrm{d}x = \tilde{q}_j\,, \tag{75}$$

where

$$\tilde{q}_j = \int_{x=0}^L p(x,t) w_j(x) dx\,. \tag{76}$$

Carrying out the same integration on Equation (72), one obtains:

$$S_j - \omega_j^2 M_j = 0\,. \tag{77}$$

Joining Equations (75) and (77):

$$M_j \frac{\mathrm{d}^2 q_j}{\mathrm{d}t^2} + M_j \omega_j^2 q_j + \int_{x=0}^L \left( c(x) + \sum_{n=1}^{b+1} \delta(x - x_n) c_{L,n} \right) \sum_{l=1}^{\infty} \frac{\mathrm{d}q_l}{\mathrm{d}t} w_l w_j \mathrm{d}x = \tilde{q}_j\,. \tag{78}$$

One can see that the damping terms are not uncoupled as in the other ones. Complete uncoupling can only be achieved if the damping is of the Rayleigh type, *i.e.* proportional to a combination of stiffness and mass terms. $\alpha$ is usually used for the mass coefficient, while $\beta$ stands for the stiffness coefficient. This is quite a common case, as one can imagine that localized dampers and the continuous damping distribution follow the same variation as the mass terms, thus $\beta$=0. In the general case:

$$
\begin{aligned}
&M_j \frac{\mathrm{d}^2 q_j}{\mathrm{d}t^2} + M_j \omega_j^2 q_j + \left(\alpha M_j + \beta S_j\right)\frac{\mathrm{d}q_j}{\mathrm{d}t} \\
&= M_j \frac{\mathrm{d}^2 q_j}{\mathrm{d}t^2} + M_j \omega_j^2 q_j + M_j\left(\alpha + \beta\omega_j^2\right)\frac{\mathrm{d}q_j}{\mathrm{d}t} = \tilde{q}_j .
\end{aligned} \tag{79}
$$

It is further assumed that $M_j\left(\alpha + \beta\omega_j^2\right) = \xi c_{cr} = 2\xi M_j \omega_j$, where $\xi$ is called the damping ratio and $c_{cr} = 2M_j\omega_j$ the critical damping. In summary:

$$
\frac{\mathrm{d}^2 q_j}{\mathrm{d}t^2} + 2\xi\omega_j \frac{\mathrm{d}q_j}{\mathrm{d}t} + \omega_j^2 q_j = \frac{1}{M_j}\tilde{q}_j = \tilde{Q}_j . \tag{80}
$$

The initial conditions also must be expanded in series:

$$
w(x,0) = \tilde{w}(x) = \sum_{j=1}^{\infty} q_j(0) w_j , \quad \frac{\mathrm{d}w}{\mathrm{d}t}(x,0) = \tilde{\tilde{w}}(x) = \sum_{j=1}^{\infty} \frac{\mathrm{d}q_j}{\mathrm{d}t}(0) w_j , \tag{81}
$$

which is not a simple task due to the orthogonality conditions. Then, Equations (80-81) can be solved by Laplace transformation (* designates the image):

$$
\begin{aligned}
&\left(-\frac{\mathrm{d}q_j}{\mathrm{d}t}(0) - p q_j(0) + p^2 q_j^*(p)\right) + \\
&2\xi\omega_j\left(-q_j(0) + p q_j^*(p)\right) + \omega_j^2 q_j^*(p) = \tilde{Q}_j^*(p)
\end{aligned} , \tag{82a}
$$

$$
\Rightarrow \quad q_j^*(p) = \frac{\frac{\mathrm{d}q_j}{\mathrm{d}t}(0) + p q_j(0) + 2\xi\omega_j q_j(0) + \tilde{Q}_j^*(p)}{p^2 + 2\xi\omega_j p + \omega_j^2} , \tag{82b}
$$

$$
p^2 + 2\xi\omega_j p + \omega_j^2 = \left(p + \xi\omega_j\right)^2 + \omega_j^2\left(1 - \xi^2\right) = \left(p + \xi\omega_j\right)^2 + \omega_{d,j}^2 , \tag{82c}
$$

$$
\begin{aligned}
q_j^*(p) = &\frac{q_j(0)\left(p + \xi\omega_j\right)}{\left(p + \xi\omega_j\right)^2 + \omega_{d,j}^2} + \left(\xi\omega_j q_j(0) + \frac{\mathrm{d}q_j}{\mathrm{d}t}(0)\right)\frac{1}{\omega_{d,j}}\frac{\omega_{d,j}}{\left(p + \xi\omega_j\right)^2 + \omega_{d,j}^2} \\
&+ \tilde{Q}_j^*(p)\frac{1}{\omega_{d,j}}\frac{\omega_{d,j}}{\left(p + \xi\omega_j\right)^2 + \omega_{d,j}^2} ,
\end{aligned} \tag{82d}
$$

$$
\begin{aligned}
q_j(t) = &q_j(0)\mathrm{e}^{-\xi\omega_j t}\cos\left(\omega_{d,j} t\right) + \frac{q_j(0)\xi\omega_j + \dot{q}_j(0)}{\omega_{d,j}}\mathrm{e}^{-\xi\omega_j t}\sin\left(\omega_{d,j} t\right) + \\
&\frac{1}{M_j\omega_{d,j}}\int_{\tilde{t}=0}^{t} \tilde{q}_j(\tilde{t})\mathrm{e}^{-\xi\omega_j(t-\tilde{t})}\sin\left(\omega_{d,j}(t - \tilde{t})\right)\mathrm{d}\tilde{t} ,
\end{aligned} \tag{82e}
$$

where Equation (82c) stands for an alternative formulation of the denominator of Equation (82b), and $\omega_{d,j} = \omega_j\sqrt{1 - \xi^2}$ is introduced as a damped frequency. However, it has nothing to do with complex frequencies of damped modes. Equation

(82e) is not restricted to subcritical damping ($\xi$<1). For a single constant moving force $P$ (exploiting Equation (76) and the fact that $p(x,t)=P\delta(x-vt)$):

$$\tilde{q}_j(t)=Pw_j(vt)\big(H(L-vt)-H(-vt)\big), \tag{83}$$

where the Heaviside function $H$ in the brackets states that this term is only valid when the force is on the beam. For homogeneous initial conditions, Equation (82e) is the same as Duhamel's integral, as expected. Sometimes, it is important to separate the final expression into homogenous and particular solutions of the ordinary differential equation (80). A simple exercise can be done for a simply supported uniform beam with no elastic foundation and homogeneous initial conditions. Then:

$$w_j=\sin\left(\frac{j\pi}{L}x\right) \quad\Rightarrow\quad \tilde{q}_j=P\sin\left(\frac{j\pi}{L}vt\right),\ M_j=\frac{\mu L}{2}, \tag{84a}$$

$$q_{P,j}(t)=q_{AP,j}\sin\left(\frac{j\pi}{L}vt\right)+q_{BP,j}\cos\left(\frac{j\pi}{L}vt\right), \tag{84b}$$

$$q_{AP,j}=\frac{P}{M_j}\frac{1}{\omega_j^2}\frac{1-\Omega_j^2}{(2\xi\Omega_j)^2+(1-\Omega_j^2)^2}, \tag{84c}$$

$$q_{BP,j}=\frac{P}{M_j}\frac{1}{\omega_j^2}\frac{-2\xi\Omega_j}{(2\xi\Omega_j)^2+(1-\Omega_j^2)^2}, \tag{84d}$$

$$q_{H,j}(t)=e^{-\xi\omega_j t}\big(q_{AH,j}\sin(\omega_{d,j}t)+q_{BH,j}\cos(\omega_{d,j}t)\big), \tag{84e}$$

$$q_{AH,j}=\frac{P}{M_j}\frac{\Omega_j}{\omega_j\omega_{d,j}}\frac{\Omega_j^2+2\xi^2-1}{(2\xi\Omega_j)^2+(1-\Omega_j^2)^2}, \tag{84f}$$

$$q_{BH,j}=\frac{P}{M_j}\frac{1}{\omega_j^2}\frac{2\xi\Omega_j}{(2\xi\Omega_j)^2+(1-\Omega_j^2)^2}, \tag{84g}$$

where $q_{P,j}$ and $q_{H,j}$ define the form of the particular and homogenous solutions, and

$$\Omega_j=\frac{\omega_{f,j}}{\omega_j}=\frac{j\pi v}{L\omega_j}, \tag{85}$$

where $\omega_{f,j}$ stands for the forced frequency. It is simple to verify that $q_{P,j}(t)=\tilde{D}(t,\tilde{t}=t)$ and $q_{H,j}(t)=-\tilde{D}(t,\tilde{t}=0)$, where $\tilde{D}(t,\tilde{t})$ is the primitive function of Duhamel's integral. This statement is valid generally.

If the restriction to linear disturbances is removed, the modal mass is defined by:

$$M_j=\int_0^L \mu(x)w_j^2(x)\mathrm{d}x+\sum_{n=1}^{b+1}\left(m_n w_j^2(x_n)+J_n\frac{\mathrm{d}w_j^2(x_n)}{\mathrm{d}x}\right). \tag{86}$$

Regarding the other option mentioned at the beginning of this section, *i.e.* when localized terms are not included in vibration modes determination, it follows:

$$\left( EI(x)\frac{\mathrm{d}^4}{\mathrm{d}x^4} + k(x) \right) w_j - \omega_j^2 \mu(x) w_j = 0, \quad \forall j \,, \tag{87}$$

meaning that the natural modes and frequencies evaluation is simpler, but final equations will be coupled with no possibility of analytical solution:

$$\mathbf{M} \cdot \ddot{\mathbf{q}}(t) + \mathbf{C} \cdot \dot{\mathbf{q}}(t) + \mathbf{K} \cdot \mathbf{q}(t) = \tilde{\mathbf{q}}(t), \tag{88}$$

where

$$M_{lj} = \delta_{lj} M_j + \sum_{n=1}^{b+1} \left( m_n w_l(x_n) w_j(x_n) + J_n \frac{\mathrm{d}w_l}{\mathrm{d}x}(x_n) \frac{\mathrm{d}w_j}{\mathrm{d}x}(x_n) \right), \tag{89a}$$

$$\begin{aligned} \mathrm{C}_{lj} = \int_{x=0}^{L} c(x) w_l w_j \mathrm{d}x + \sum_{n=1}^{b+1} \Bigg( & c_{L,n} w_l(x_n) w_j(x_n) + c_{LR,n} w_l(x_n) \frac{\mathrm{d}w_j}{\mathrm{d}x}(x_n) \\ & + c_{RL,n} \frac{\mathrm{d}w_l}{\mathrm{d}x}(x_n) w_j(x_n) + c_{R,n} \frac{\mathrm{d}w_l}{\mathrm{d}x}(x_n) \frac{\mathrm{d}w_j}{\mathrm{d}x}(x_n) \Bigg), \end{aligned} \tag{89b}$$

$$\begin{aligned} K_{lj} = \delta_{lj} M_j \omega_j^2 + \sum_{n=1}^{b+1} \Bigg( & k_{L,n} w_l(x_n) w_j(x_n) + k_{LR,n} w_l(x_n) \frac{\mathrm{d}w_j}{\mathrm{d}x}(x_n) \\ & + k_{RL,n} \frac{\mathrm{d}w_l}{\mathrm{d}x}(x_n) w_j(x_n) + k_{R,n} \frac{\mathrm{d}w_l}{\mathrm{d}x}(x_n) \frac{\mathrm{d}w_j}{\mathrm{d}x}(x_n) \Bigg). \end{aligned} \tag{89c}$$

This formulation includes springs and dampers with the additional specifications *LR* and *RL*, *i.e.* a spring (damper) in which the reaction to applied rotation (rotational velocity) is a force and one in which the reaction to applied displacement (velocity) is a moment. In other words, any additional member characterized by a full, possibly non-symmetric 2x2 matrix, can be added this way. Similar extensions could be done for concentrated masses.

Extending the analysis to the originally assumed T-R beam, it is convenient to write Equations (40-41) in the first order state-space form (similarly as in [22]):

$$\begin{bmatrix} G\tilde{A} - EI\dfrac{\partial^2}{\partial x^2} & -G\tilde{A}\dfrac{\partial}{\partial x} & 0 & 0 \\ G\tilde{A}\dfrac{\partial}{\partial x} & k-\left(N+k_p\right)\dfrac{\partial^2}{\partial x^2} - G\tilde{A}\dfrac{\partial^2}{\partial x^2} & 0 & 0 \\ 0 & 0 & -\mu r^2 & 0 \\ 0 & 0 & 0 & -\mu \end{bmatrix} \cdot \begin{Bmatrix} \psi(x,t) \\ w(x,t) \\ \vartheta(x,t) \\ \tau(x,t) \end{Bmatrix} + \tag{90}$$

$$\begin{bmatrix} 0 & 0 & \mu r^2 & 0 \\ 0 & c & 0 & \mu \\ \mu r^2 & 0 & 0 & 0 \\ 0 & \mu & 0 & 0 \end{bmatrix} \cdot \frac{\partial}{\partial t} \begin{Bmatrix} \psi(x,t) \\ w(x,t) \\ \vartheta(x,t) \\ \tau(x,t) \end{Bmatrix} = \begin{Bmatrix} 0 \\ p(x,t) \\ 0 \\ 0 \end{Bmatrix},$$

where:

$$\vartheta(x,t) = \frac{\partial}{\partial t}\psi(x,t),\ \tau(x,t) = \frac{\partial}{\partial t} w(x,t). \tag{91}$$

Several simplifications are introduced here. The beam characteristics $x$-dependence is not written. The localized disturbances could be accounted for by augmented operators, similarly as in [21], but are disregarded for simplicity. The Pasternak damping term is neglected, in order to ensure that the operator matrices in Equation (90) are self-adjoint. Equation (90) allows for recasting the eigenvalues problem into linear equations, but in the following, mostly generalized coordinates solution will be analysed. Two orthogonality relations for damped vibration modes are derived as:

$$\begin{aligned} &\int_{x=0}^{L} \Bigg( \psi_k \left( G\tilde{A}\psi_j - EI\frac{d^2\psi_j}{dx^2} - G\tilde{A}\frac{dw_j}{dx} \right) \\ &+ w_l \left( G\tilde{A}\frac{d\psi_j}{dx} + kw_j - \left(N+k_p\right)\frac{d^2 w_j}{dx^2} - G\tilde{A}\frac{d^2 w_j}{dx^2} \right) \\ &+ \omega_l\omega_j\mu r^2\psi_l\psi_j + \omega_l\omega_j\mu w_k w_j \Bigg) \mathrm{d}x = \delta_{lj} S_j, \end{aligned} \tag{92a}$$

$$\int_{x=0}^{L} \left( i\mu r^2\left(\omega_l+\omega_j\right)\psi_l\psi_j + i\mu\left(\omega_l+\omega_j\right)w_k w_j + c w_l w_j \right)\mathrm{d}x = \delta_{lj} T_j, \tag{92b}$$

connected by

$$S_j + i\omega_j T_j = 0, \tag{93}$$

which allows introduction of the modal mass in a generalized form as:

$$S_j = -i\omega_j T_j = 2\omega_j^2 M_j,\ M_j = -iT_j/\left(2\omega_j\right) \tag{94a}$$

$$M_j = \int_{x=0}^{L} \left( \mu w_j^2 + \mu r^2 \psi_j^2(x) + \frac{c}{2i\omega_j} w_j^2 \right) dx. \tag{94b}$$

Expanding the unknown functions in modal series:

$$\begin{Bmatrix} \psi(x,t) \\ w(x,t) \\ \vartheta(x,t) \\ \tau(x,t) \end{Bmatrix} = \sum_{j=1}^{\infty} q_j(t) \begin{Bmatrix} \psi_j(x) \\ w_j(x) \\ \vartheta_j(x) \\ \tau_j(x) \end{Bmatrix} \tag{95}$$

and exploiting Equation (90), one obtains a first order modal equation of motion:

$$S_j q_j + T_j \frac{\mathrm{d}q_j}{\mathrm{d}t} = \tilde{q}_j \,, \tag{96}$$

where $\tilde{q}_j$ is given by Equation (83) for a single moving force $P$. Equation (96) can be normalized into:

$$\frac{\mathrm{d}}{\mathrm{d}t} q_j - i\omega_j q_j = \frac{-iP}{2\omega_j M_j} w_j(vt). \tag{97}$$

This formulation can be used to show the difference between expansions into damped or undamped modes. But probably, the only analytical solution of complex frequencies that is possible for simply supported uniform E-B beam without any additional effect, is:

$$\omega_{j,l} = i\frac{c}{2\mu} \pm \sqrt{\left(\frac{j\pi}{L}\right)^4 \frac{EI}{\mu} - \left(\frac{c}{2\mu}\right)^2} \,,\ l=1,2. \tag{98}$$

The solution of Equation (97) can be written as:

$$q_{j,l} = \frac{1}{2i\omega_{j,l} M_{j,l}} \int_{\tilde{t}=0}^{t} \tilde{q}_j(\tilde{t}) \mathrm{e}^{i\omega_{j,l}(t-\tilde{t})} \mathrm{d}\tilde{t} \,,\ l=1,2. \tag{99}$$

Exploiting Equations (94b) and (98):

$$2i\omega_{j,1} M_{j,1} = i\mu L \sqrt{\left(\frac{j\pi}{L}\right)^4 \frac{EI}{\mu} - \left(\frac{c}{2\mu}\right)^2} = 2iM_j \omega_{d,j} \,, \tag{100a}$$

$$2i\omega_{j,2} M_{j,2} = -i\mu L \sqrt{\left(\frac{j\pi}{L}\right)^4 \frac{EI}{\mu} - \left(\frac{c}{2\mu}\right)^2} = -2iM_j \omega_{d,j} \,, \tag{100b}$$

where $M_j$ and $\omega_{d,j}$ correspond to the values derived for expansion governed by undamped modes. One can join the solutions into:

$$\begin{aligned} q_j = q_{j,1} + q_{j,2} &= \frac{1}{M_j \omega_{d,j}} \int_{\tilde{t}=0}^{t} \tilde{q}_j(\tilde{t}) \mathrm{e}^{-\xi\omega_j(t-\tilde{t})} \frac{\mathrm{e}^{\omega_{d,j}(t-\tilde{t})} - \mathrm{e}^{-\omega_{d,j}(t-\tilde{t})}}{2i} \mathrm{d}\tilde{t} \\ &= \frac{1}{M_j \omega_{d,j}} \int_{\tilde{t}=0}^{t} \tilde{q}_j(\tilde{t}) \mathrm{e}^{-\xi\omega_j(t-\tilde{t})} \sin\left(\omega_{d,j}(t-\tilde{t})\right) \mathrm{d}\tilde{t} \,, \end{aligned} \tag{101}$$

and obtain the previous solution from Equation (82e), as expected. The case presented exhibits only real-valued vibration modes, even for complex frequencies. More complicated cases can be found in [21]. The general case is quite difficult to solve, but when discretization is implemented, the complex frequencies and complex vibration modes can be solved within reasonable difficulty [23].

# 5 Internal forces, inertial and other effects

Determination of beam bending moment and shear force can be accomplished using Equations (46) and (47). However, when a concentrated moving force is considered, there is a discontinuity in the shear force, *i.e.* a discontinuity in the derivative of the bending moment. This dictates that for reasonable accuracy, many modes, generally more than for the deflection representation, are necessary. An alternative rearrangement derived directly from the governing equations is presented in [24].

Until now, the effect of load inertia was disregarded. If it is employed, the right hand side of the governing Equation (41) must be altered into

$$p - \frac{p}{g}\frac{\partial^2 w}{\partial t^2}, \tag{102}$$

where $g$ is the acceleration of gravity. For a single moving force $P$, it means that:

$$\left(P - \frac{P}{g}\frac{\partial^2 w}{\partial t^2}\right)\delta(x - vt). \tag{103}$$

A classical solution to this problem is presented in [25]. An undamped E-B beam with no additional effects is considered. The modal expansion is accomplished over undamped vibration modes determined without the moving mass contribution. The moving mass effect is then moved to the left hand side of the governing equation. This leads to a system of uncoupled equations for the modal coordinates similar to Equations (89). Here it holds:

$$\mathbf{M}\cdot\ddot{\mathbf{q}}(t) + \mathbf{K}\cdot\mathbf{q}(t) = \tilde{\mathbf{q}}(t), \tag{104}$$

where

$$M_{lj} = \delta_{lj}M_j + Pw_l(vt)w_j(vt)\sqrt{M_l M_j}\,/\,g\,, \tag{105a}$$

$$K_{lj} = \delta_{lj}M_j\omega_j^2\,. \tag{105b}$$

Additional effects can be added in the same way as in Equations (89). Extension of this solution to beams on an elastic foundation does not provide correct results, because the terms representing the foundation mass were neglected (see Section 3.1). An approximation can be done by adding a representative soils mass to the beam mass per unit length. Alternative approaches for solving the moving mass problem employ expansion of Equation (103) in series and neglecting insignificant terms.

As a closing remark, it is necessary to highlight that, when the beam deforms, the conventional elastic foundation can sustain both compression and tension. This model was probably motivated more by the desire for mathematical simplicity than by physical reality. The steady state deformation of an infinite beam on a tensionless elastic foundation under a moving load was first studied in [26].

# 6 Conclusions

In this chapter several aspects related to dynamic analysis of beam structures under moving loads were summarized. Emphasis has been placed on the modal expansion method and a few examples were related to high-speed railways. The concept of the dynamic stiffness matrix was posted as a general principle for finite, semi-infinite and infinite beams. The importance of governing equations reformulations, ensuring the orthogonality of natural vibration modes, has been discussed in detail. Some developments are new; review and summary of published works is far from complete due to a considerable amount of studies that have been published on this subject.

# Acknowledgements

The work was partially supported by the project grant PTDC/EME-PME/01419/2008: “SMARTRACK - SysteM dynamics Assessment of Railway TRACKs: a vehicle-infrastructure integrated approach” of Fundação para a Ciência e a Tecnologia of the Portuguese Ministry of Science and Technology.

# References

[1] A.N. Krylov, (A.N. Kriloff), “Über die erzwungenen Schwingungen von gleichformigen elastichen Stäben”, Mathematische Annalen, 61, 211-234, 1905 (in German).

[2] S.P. Timoshenko, “Forced vibration of prismatic bars”, Izvestiya Kievskogo politekhnicheskogo instituta (in Russian), 1908; Erzwungene Schwingungen prismatischer Stabe, Zeitschrift für Mathematik und Physik 59 (2): 163–203, 1911 (in German).

[3] C.E. Inglis, A Mathematical Treatise on Vibration in Railway Bridges, The Cambridge University Press, Cambridge, 1934.

[4] A.N. Lowan, “On transverse oscillations of beams under the action of moving variable loads”, Philosophical Magazine, Series 7, 19 (127), 708–715, 1935.

[5] V. Koloušek, Dynamics of Civil Engineering Structures—Part I: General problems, 2nd ed.—Part II: Continuous Beams and Frame Systems, 2nd ed—Part III: Selected Topics, SNTL, Prague, 1967, 1956, 1961 (in Czech.). Dynamics in engineering structures, Academia, Prague, Butterworth, London, 1973.

[6] L. Frýba, Vibration of Solids and Structures under Moving Loads, Research Institute of Transport, Prague (1972), 3rd edition, Thomas Telford, London, 1999.
[7] S.P. Timoshenko, Statical and dynamical stresses in rails, Proceedings of the 2nd International Congress for Applied Mechanics, Zürich (Switzerland), 12-17 September 1926, 407-418.
[8] J.T. Kenney Jr., Steady-state vibrations of beam on elastic foundation for moving load. ASME Journal of Applied Mechanics, 21: 359-364, 1954.
[9] L. Frýba, Infinite Beam on an Elastic Foundation Subjected to a Moving Load (in Czech). Aplikace Matematiky, 2 (2): 105-132, 1957.
[10] J.A. Cottrell, A. Reali, Y. Bazilevs, T.J.R. Hughes, "Isogeometric analysis of structural vibrations", Computer Methods in Applied Mechanics and Engineering, 195, 5257-5296, 2006.
[11] Release R2007a Documentation for MATLAB, The MathWorks, Inc., 2007.
[12] Release 11 Documentation for MAPLE, Maplesoft a division of Waterloo Maple, Inc., 2007.
[13] Z. Dimitrovová, "A general procedure for the dynamic analysis of finite and infinite beams on piece-wise homogeneous foundation under moving loads", Journal of Sound and Vibration, 329, 2635–2653, 2010.
[14] J. Máca, "Dynamic analysis of plates on elastic foundation", Proceedings of the 4th International Conference on Structural Dynamics, EURODYN2002, H. Grundmann and G.I. Schueller (eds.), Munich, Germany, 2-5 September 2002, pp.887-892.
[15] G. Karami, P. Malekzadeh, S.A. Shahpari, "A DQEM for vibration of shear deformable nonuniform beams with general boundary conditions", Engineering Structures, 25, 1169–1178, 2003.
[16] Y-H. Chen, Z-M. Shiu, "Resonant curves of an elevated railway to harmonic moving loads", International Journal of Structural Stability and Dynamics, 4 (2), 237-257, 2004.
[17] Y-H. Chen, J-T. Sheu, "Beam length and dynamic stiffness", Computer Methods in Applied Mechanics and Engineering, 129, 311-318, 1996.
[18] Y-H. Chen, Y-H. Huang, "Dynamic stiffness of infinite Timoshenko beam on viscoelastic foundation in moving co-ordinate", International Journal For Numerical Methods In Engineering, 48, 1-18, 2000.
[19] Z. Dimitrovová, J.N. Varandas, Critical velocity of a load moving on a beam with a sudden change of foundation stiffness: Applications to high-speed trains. Computers & Structures, 87: 1224–1232, 2009.
[20] L. Meirovitch, Computational methods in structural dynamics, Sijthoff & Noordhoff, 1980.
[21] B. Yang, X. Wu, "Transient response of one-dimensional distributed systems: a closed form eigenfunction expansion realization", Journal of Sound and Vibration, 208(5), 763-776, 1997.
[22] S. Krenk, Complex modes and frequencies in damped structural vibrations. Journal of Sound and Vibration, 270, 981-996, 2004.

[23] J.C.O. Nielsen, J. Oscarsson, “Simulation of dynamic train–track interaction with state-dependent track properties”, Journal of Sound and Vibration, 275, 515-532, 2004.
[24] M. Zehsaz, M.H. Sadeghi, A. Ziaei Asl, Dynamic response of railway under a moving load. *Journal of Applied Sciences,* 9 (8), 1474-1481, 2009.
[25] J.E. Akin, M. Mofid, Numerical solution for response of beams with moving mass. *ASCE Journal of Structural Engineering*, 115: 120–31, 1989.
[26] J. Choros, G.G. Adams, A steadily moving load on an elastic beam resting on a tensionless Winkler foundation. ASME Journal of Applied Mechanics, 46: 175-180, 1979.